Applied Energy 221 (2018) 358–373

Contents lists available at ScienceDirect

Applied Energy

journal homepage: www.elsevier.com/locate/apenergy

Assessment of forecasting methods on performance of photovoltaic-battery systems

G.B.M.A. Litjens*, E. Worrell, W.G.J.H.M. van Sark

Copernicus Institute of Sustainable Development, Utrecht University, PO Box 80.115, 3508TC Utrecht, The Netherlands

HIGHLIGHTS

- Development and assessment of forecast methods and predictive control strategy.
- Strategies tested on 48 residential and 42 commercial PV-battery systems.
- Predictive control greatly decreases feed-in losses with minor loss of self-consumption.
- Recommended to customize forecast methods based on PV system boundary conditions.

ARTICLE INFO

Keywords:
PV-battery systems
Battery control strategies
Forecasting methods
Self-consumption
Feed-in limit
Storage revenues

ABSTRACT

Photovoltaic (PV) systems are increasingly deployed on buildings in urban areas, causing additional power flows and frequency fluctuation on the low voltage electricity grid. Control strategies for PV-battery energy storage systems (BESS) assist in reducing power flows to the grid and improve the self-consumption of PV generated electricity. Therefore, these control strategies require accurate forecasts of PV electricity production and electricity consumption. We developed and assessed relatively simple forecasting methods using 5 min resolution data, to predict the PV yield and to forecast electricity consumption for one year. We used these forecasts with a predictive control strategy to increase PV self-consumption, decrease curtailment losses and improve BESS revenues. Electricity demand patterns of 48 residential and 42 commercial Dutch buildings were used. PV yield forecast methods that uses predicted weather data shows the lowest forecast error. The best performing forecast method for predicting energy consumption of residential buildings requires historical energy consumption data of the previous seven days. Commercial systems require historical energy consumption of the previous weekday. Significant reduction in curtailment losses is achieved using predictive control strategies, especially in combination when clear-sky radiation data is used to forecast PV yield. Similar self-consumption rates were found for predictive control as for real-time control. This indicates that reduction of curtailment loss can be combined while maintaining the level of PV self-consumption. Revenues from battery storage are increased by forecast methods and are highly dependable on boundary condition of a PV-battery system, such as the feed-in limit (FIL) and the feed-in tariff. Therefore, we recommend customizing battery control strategies based on these system boundaries conditions to improve energy storage potential.

1. Introduction

Optimal integration of photovoltaics (PV) produced energy in the low voltage electricity grid supports cost effective transition towards a fully sustainable energy system. One way to enhance PV system integration is using battery energy storage systems (BESS). PV systems with batteries enable the use of PV produced energy at later moments. Subsequently, more locally produced energy is used and thus PV self-consumption increased. PV-battery systems can reduce the impact on low voltage electricity grids when using algorithms that properly reduce PV peak power. Consequently, investments in new cables and transformers can be deferred to later years, thus saving on necessary update investments. Higher PV self-consumption lower grid losses and potentially reduces CO_2 emissions from fossil-based backup power generation, especially when curtailment of PV energy is avoided [1]. Another important economic incentive for self-consumption is the absolute difference in consumption tariff and feed-in tariff. This difference indicates the economic value of the self-consumed electricity. Due to all these benefits, PV self-consumption is becoming a major incentive for continued PV market growth in urban areas [2]. Subsequently, policies

* Corresponding author.
E-mail addresses: g.b.m.a.litjens@uu.nl (G.B.M.A. Litjens), e.worrell@uu.nl (E. Worrell), w.g.j.h.m.vansark@uu.nl (W.G.J.H.M. van Sark).

https://doi.org/10.1016/j.apenergy.2018.03.154
Received 16 January 2018; Received in revised form 28 March 2018; Accepted 30 March 2018
Available online 17 April 2018

Nomenclature

Abbreviations

AC	alternating current
BESS	battery energy storage systems
CEC	California Energy Commission
DC	direct current
FIL	feed-in limit
PC	predictive control
PV	photovoltaics
RC	real-time control
RER	relative electricity revenue
SOC	state of charge
SPR	sales to purchase ratio
TSO	transmission system operator

Forecast methods

D-PD	demand pattern using previous day
D-PW	demand pattern using average of previous week
D-PWD	demand pattern using previous weekday
PV-CS	PV pattern using clear-sky radiation
PV-PD	PV pattern using previous day
PV-PW	PV pattern using average of previous week
PV-WX	PV pattern using weather prediction data

Performance indicators

Δ_{se}	performance indicator difference between a forecast scenario and the exact forecast [%p]
CLR	curtailment loss ratio [%]
MAPE	mean absolute percentage error [%]
nMBE	normalized mean bias error [%]
nRMSE	normalized root mean square error [%]
SCR	self-consumption ratio [%]
SRR	storage revenue ratio [%]

Time-independent parameters

Δt	5 min
$RER_{PV\text{-}B}$	relative electricity revenue of a PV system with BESS installed
RER_{PV}	relative electricity revenue of a PV system
π_{cons}	consumption tariff [€/W h]
π_{feed}-in	feed-in tariff [€/W h]
$E_{B\,max}$	maximum battery state of charge [W h]
$E_{B\,min}$	minimum battery state of charge [W h]
E_{PV}	PV produced energy [W h]
E_{RIE}	reduced imported energy [W h]
E_{SC}	self-consumed energy [W h]
E_{SE}	sold energy [W h]
n	number of timesteps
$P_{B\,inv\,max}$	battery inverter rating [W]
P_{FIL}	power feed-in limit [W]
t	time

Time-dependent parameters

$\Delta E_{B\,pot}$	battery charge or discharge energy potential [W h]
ΔE_B	battery charge or discharge energy [W h]
η_{charge}	battery charge efficiency [%]
$\eta_{discharge}$	battery discharge efficiency [%]
$E_{B,t}$	battery state of charge [W h]
$E_{B\,res\,pot}$	potential battery storage capacity reserved [W h]
$E_{B\,res}$	storage state of charge reserved [W h]
$E_{FIL\,loss}$	lost PV energy due to feed-in limitation [W h]
P_{actual}	actual power of PV yield or demand [W]
P_{FC}	forecasted power of PV yield or demand [W]
$P_{B\,inv}$	battery inverter load [W]
$P_{B\,pot}$	battery load potential [W]
$P_{B\,res}$	battery charge capacity reserved [W]
P_B	battery load [W]
P_{charge}	power charged to the battery [W]
$P_{D\,FC}$	forecasted electricity demand [W]
$P_{direct\,SC}$	direct self-consumed power [W]
P_D	electricity demand [W]
$P_{FIL\,FC}$	forecasted feed-in power exceeding the feed-in limited [W]
$P_{FIL\,loss}$	power loss due to the feed-in limit [W]
P_G	load from or to the grid [W]
P_{pot}	load potential [W]
$P_{PV\,FC}$	forecasted PV production [W]
P_{PV}	PV produced power [W]
P_R	residual power flow [W]

supporting PV self-consumption are developed and implemented in multiple countries [3].

Feed-in limits (FIL) restrict the maximum power flow which is exported back to the electricity grid. These are usually given as a percentage of the installed PV system capacity. Therefore, high PV peak power is avoided on the local electricity grid which increases power quality in low voltage grid. Electricity from PV systems that is not exported nor used is lost, also known as curtailment losses. Consequently, financial support schemes are developed that support the storage of PV peak power. For instance, PV-battery systems in Germany can apply for financial support when the power flow back to the grid is limited to 0.5 kW for each kWp of installed PV capacity [4]. Furthermore, a lower feed-in power results in a lower grid connection and potentially a reduced grid connection fee. In choosing the best charging and discharging times, forecasts of PV electricity production and electricity consumption are essential. Therefore the curtailment losses will be reduced and the level of PV self-consumption can be maintained.

1.1. Literature review

Several studies examined forecasting methods for PV yield and electricity consumptions. A comprehensive overview of PV forecasting methods has been given in a recent review [5]. This study divided forecasting methods into probabilistic forecasting and deterministic forecasting. Most of these studies used historical measured data and/or weather data. For example, PV forecast methods have been developed that used power output of neighbouring PV systems [6]. Also, various methods have been proposed to demand forecasting in a recent literature review, which made a division between statistical based and artificial intelligence based models [7]. Time-of-use models have been proposed to predict energy consumption based on the user and appliances within a building [8].

A limited amount of studies assess the influence of these forecasts on the performance of control strategies for PV-battery systems. A recent review found that control strategies using forecasting data with feed-in power limits showed manageable curtailment losses. These strategies are promising, especially when feed-in limitations are further reduced [9]. A study including a German residential demand profile has shown

that 26% more PV capacity can be added to the grid by using PV-battery systems with persistence forecast algorithms [10]. A Swiss study assessed a control strategy that used forecasted PV power production under clear-sky conditions for residential systems. This strategy has a shown a similar performance in reducing curtailment losses as an exact PV forecast [11]. Also, control strategies using variable time horizons from historical PV production data have been proposed and assessed [12–16]. These control strategies used diverse methods to determine the optimal battery state for each time step. Moreover, Markov chain-based forecasting approaches have been suggested for optimizing battery control strategies [17].

The economic profitability of PV-battery systems depends on the aim of the used control strategy. Storage of PV electricity to mitigate over-voltage problems could be economically viable, if feed-in tariffs are higher than off-peak consumption tariffs [18]. However, considering that a large share of the consumption tariff consists of taxes, a feed-in tariff higher than a consumption tariff seems not plausible. Control strategies that included a minimization of dwell times for high battery state of charges (SOC) could improve battery life time [19]. For example, a strategy that only stored PV energy required to meet the energy demand for the following night could be used to achieve this aim [20]. Also, forecast based strategy reduced the electricity bill of German households especially when a feed-in limit is present[21].

The literature illustrates that performance of control strategies for BESS is directly influenced by the accuracy of the forecasted energy consumption of a building and PV production. Furthermore, a recent review study identified that the economic impact of forecasting has not been studied in depth. More knowledge on the influence of the combination of electricity demand and PV production forecast methods is required to understand its impact on the PV-battery system. The influence of combining forecast methods on performance of PV-battery systems with different energy demand patterns is not well known. Most studies use a limited number of residential demand patterns. Also, studies that assess the performance of commercial PV-battery systems, for example for office buildings, were not found.

1.2. Research aim

The aim of this study is to assess the influence of PV and demand pattern forecasting methods on the performance of the PV-battery system, using a predictive control strategy. This strategy aims to reduce curtailment losses without reducing the self-consumption of the PV-battery system. Previous studies mainly used single or a few demand patterns to assess forecast methods. Our paper goes beyond these studies by using 48 residential and 42 commercial electricity consumption patterns from a full year (2013) to test our forecasting methods. We present the results in the form of distributions and statistics which give realistic prognoses.

Most studies asses the performance of PV-battery systems using a single forecast method, or assume a perfect forecast. Besides sophisticated models, for example Markov chain models or artificial neuron network, are commonly used to predict system behaviour. We aimed to develop simple statistical based forecasting methods to use in a battery control strategy. The developed methods are easily applied to real-time applications and require less computational power and data storage space. We believe this will increases the implementation potential over the more sophisticated models.

Four methods to predict the PV yield and three methods to forecast energy consumption of residential and commercial (office) buildings were developed and assessed. A novel battery capacity reservation algorithm was developed that uses forecasting data. This algorithm updates the battery capacity reservation based on the predicted demand and PV yield for each 5 min for each day. Moreover, it is not dependent on location or seasonal influences, therefore widely applicable. The sensitivity of used forecast methods on the PV-battery system performance is assessed for different PV sizes, battery storage and battery inverter ratings, feed-in limitations and electricity tariffs.

Our obtained results provide insights on PV and demand pattern forecasting impact on PV-battery systems, especially for locations in Western Europe. Large variety in modelled systems and our sensitivity study provides an overview of the variety of results. Especially, the direct comparison between residential and commercial systems shows the potential for each sector. This knowledge will help developers of BESS control algorithms to improve their products. In addition, distribution system operators gain a better understanding of the impact of feed-in limit on the performance of PV-battery systems. This will help policy makers making better decisions on strategies to implementing PV-battery systems in urban areas.

The remainder of this paper is structured according to the following format. Section 2 explanation the used data, developed forecasting methods and battery control strategies, and battery performance indicators. Section 3 presents the results on the performance of the forecast methods and the battery control strategies. In Section 4 the sensitivity of the PV-battery system parameters were assessed. Section 5 discusses the results and provides recommendations for further research and implementation of the developed strategies. The paper closes with the key conclusion in Section 6.

2. Methods

The explanation of the methodology consists of four parts. Section 2.1 describes the used PV yield and electricity consumption patterns. Section 2.2 explains the developed forecasting methods to predict the PV production and electricity consumption. Also the forecast error metrics are explained. Section 2.3 explains the used battery storage model and control strategies. Section 2.4 defines the indicators used to assess the impact of these forecast methods and battery control strategies on the performance of the PV-battery systems.

2.1. Real-time patterns

2.1.1. PV yield pattern

A PV yield pattern containing AC power was generated using the PVLIB (v0.5.0) model for De Bilt in the Netherlands (52.11N, 5.18E), which is the location of the Royal Netherlands Meteorological Institute (KNMI). The Python package PVLIB contains validated atmospheric functions and PV system performance models and is open source [22]. Solar radiation, ambient temperature, dew point temperature, wind speed and atmospheric pressure data was measured by the KNMI. The time interval of measurements was 10 min for radiation and one hour for the remaining weather parameters. All weather parameters were resampled to a 5 min interval using linearly interpolation. These parameters were used to model a PV pattern with a 5 min time step.

The PV yield pattern was modelled for a south oriented PV system (180° azimuth) with a module tilt of 35°. The PV system model used PV module parameters from the Sanyo HIP-225HDE1. This PV technology shows stable performance under varying Dutch weather conditions and has a relative low temperature coefficient [23]. The Enphase Energy M210 PV inverter with 95.5% California Energy Commission (CEC) efficiency was used to convert direct current (DC) power PV output to alternating current (AC) power. The maximum DC input power of this inverter is lower than the maximum output of the module, thus the PV inverter is slightly underrated. But, a larger inverter will have a reduced efficiency at low DC power inputs. Considering the Dutch weather conditions with many cloudy days, this will result in lower PV power output. We estimated a 0.6 kW h or 0.07% additional power loss caused by the clipping of the DC module power. A 5% larger inverter decreases these clipping losses, yet the annual yield is lower with 0.3 kW h. The PV yield pattern was scaled to a performance ratio of 85%, which corresponds with good performing PV systems in the Netherlands [24]. The modelled PV system yield was 956 kW h/kW for 2013. The standby consumption of the inverter was 5.8 kW h, resulting in a net PV yield of

949 kW h/kWp. The PV pattern was linearly scaled to the PV system sizes used throughout this study.

2.1.2. Demand patterns

Residential demand patterns were derived from measurements conducted by a Dutch distribution system operator between 2012 and 2014, which are available online [25]. 48 residential demand patterns, with different dwelling types, were selected for 2013. Commercial electricity consumption of 42 buildings, mainly offices, was measured in 2013. The selected residential and commercial demand patterns have a data availability of 100% and were used in a previous study [26]. Both residential and commercial demand patterns were measured at 15 min time resolution. Subsequently, these patterns were linearly resampled to match the PV yield pattern. Hence, all used patterns have an interval of 5 min and cover the full year of 2013.

Fig. 1 presents the distribution of the annual electricity demand for each hour and each month of 2013 using violin plots. These plots combine a box-whisker plot with a kernel density plot, providing a quick indication of the distribution of a dataset [27]. The wider sections of a violin plot indicate a higher probability whereas the smaller parts show a lower probability of the value. The electricity consumption was normalized to an annual electricity consumption of 1MW h. Residential electricity consumption is lower during the afternoon but higher in the evening, compared to commercial energy consumption. The distribution range of residential consumption is larger in the evening hours, due to the greater variation in user behaviour. Monthly electricity consumption shows a larger variation for residential buildings than commercial buildings. Residential buildings are occupied less in the summer months due to longer daytimes and holidays, if compared to winter months. Also commercial systems show a reduced consumption in August and December, mainly due holidays. Heat demand of the buildings was not provided by electricity, therefore limiting the influence of temperature on the electricity consumption.

2.2. Forecasting methods

Forecasted PV and demand patterns were developed and assessed. These patterns should be available prior to the start of each day of the year to be useable for the predictive forecast strategies. Four methods were used to obtain the forecasted PV yield.

1. Use the PV pattern of the previous day (PV-PD).
2. Calculate the average PV pattern from the previous week (PV-PW).
3. Use weather prediction data for the coming day to model the PV pattern (PV-WX).
4. Use clear-sky radiation to model the PV pattern (PV-CS).

The average PV pattern from the previous weekdays was constructed by taking the mean of each 5 min of each day. For example, the value from time step 12.00 is the average of the values from this similar time step of the previous seven days. Forecasted weather parameters were obtained for the next 24 h with a 3 h time step from the European Centre for Medium-Range Weather Forecasts ECMWF for location De Bilt (Netherlands) [28]. This dataset contains all weather parameters required to model the PV yield pattern with the PV model and was linear interpolate to a time interval of 5 min. The clear-sky radiation was modelled using the Ineichen clear-sky model [29]. The remaining weather parameters for the clear-sky PV pattern were set as constant values. These constants are a temperature of 12 °C, a dew point temperature of 12 °C, windspeed of 1 m/s, and a pressure of 101,325 Pa. Forecasted demand patterns were generated using three methods, all requiring historically measured demand.

1. Use the demand profile of the previous day (D-PD).
2. Use the demand profile of the previous weekday or weekend day (D-PWD).
3. Calculate the average profile from the previous seven days (D-PW).

The demand of the previous weekday or weekend day was found by selecting the demand pattern measured from exactly seven days ago. The average profile of the previous seven days was determined using a similar method as described for averaging the PV patterns for seven days.

2.2.1. Forecast performance indicators

The accuracy of forecasted PV yield and demand patterns related to actual patterns was assessed using three error metrics: normalized root mean square error (nRMSE), normalized mean bias error (nMBE) and mean absolute percentage error (MAPE). These are the most used metrics to evaluate forecasts [5]. The nRMSE and MAPE assess the magnitude and volatility of the difference between actual (P_{actual}) and

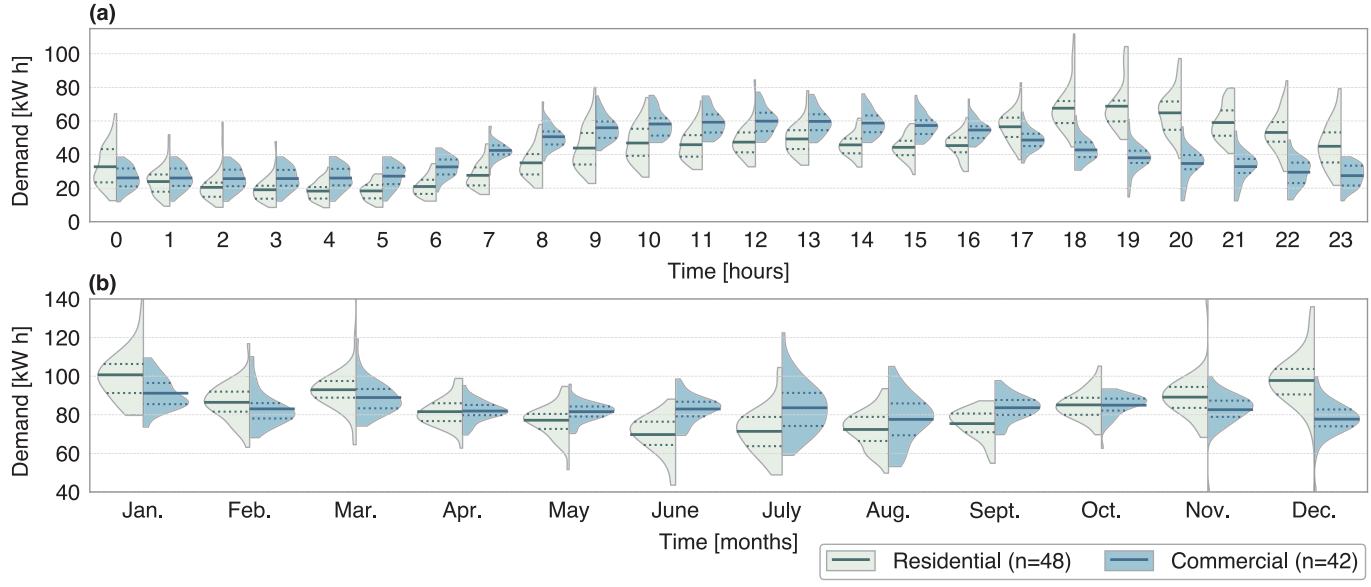

Fig. 1. Hour of the day (a) and monthly (b) electricity consumption shown using violin plots. Distribution of residential demand patterns is shown on the left side of the violin and commercial demand patterns on the right side of the violin. The demand patterns were normalized to an annual energy consumption of 1 MW h. Mean values of the distributions are marked by solid lines, and 25% and 75% percentiles are indicated by dotted lines.

forecasted pattern (P_{FC}). The nMBE evaluates if the forecast methods overestimate or an underestimate the generated power. The nRMSE and nMBE were normalized with the maximum power output from the actual forecast. The nRMSE, MAPE and nMBE are given in Eqs. (1)–(3) respectively, where n indicates the number of total time steps.

$$\text{nRMSE} = \frac{\sqrt{\frac{100\%}{n}\cdot\sum_{t=1}^{n}(P_{FC,t}-P_{actual,t})^2}}{\text{Max}(P_{actual})} \quad (1)$$

$$\text{MAPE} = \frac{100\%}{n}\sum_{t=1}^{n}\left|\frac{P_{FC,t}-P_{actual,t}}{\text{Max}(P_{actual})}\right| \quad (2)$$

$$\text{nMBE} = \frac{\frac{100\%}{n}\cdot\sum_{t=1}^{n}(P_{FC,t}-P_{actual,t})}{\text{Max}(P_{actual})} \quad (3)$$

2.3. Battery control strategies

Real-time and forecasted PV patterns were assessed using a PV-battery model. This model assessed two control strategies and was developed in Python (v3.5). The strategies were modelled for the residential and commercial systems for the year 2013. A model step of 5 min was selected to match the time steps of input patterns.

- Real-time control (RC). This strategy uses actual measured energy PV production and energy consumption to control the battery energy storage systems. No forecasts are required.
- Predictive control (PC). This strategy uses forecasted energy production and forecasted energy consumption to reduce the curtailment losses. A forecasted PV and demand pattern before the start of the day is required.

Two PV-battery systems architectures, AC-coupled and DC-coupled, are mainly used. In an AC-coupled system, the battery storage is connected with a battery inverter to the electricity grid. The PV array is connected with a PV inverter to the electricity grid and a conversion step from DC to AC power is required. If the battery is charged then the AC power is converted back to DC. An overview of the power flows within AC-coupled systems is shown in Fig. 2. In a DC-coupled system, the battery is connected directly to the PV system inverter, and no conversion to AC is needed. A charge controller is required to match the PV voltage output within the boundaries of the battery voltage input. In this study an AC-coupled lithium-based battery system is assumed. AC-coupled systems are suitable for retrofit existing PV systems with battery storage and therefore widely used in other studies [30].

The battery inverter converts the AC power to a DC power as input for the battery. The conversion efficiencies depend on the input power and were obtained from a battery inverter efficiency curve. This curve was constructed using efficiency parameters of the SMA Sunny Boy Storage inverter and has efficiency steps of 0.01% [31]. The modelled efficiency curve has a CEC inverter efficiency of 96.4%. A constant battery charging and discharging efficiency of 96% was assumed. This leads to a DC input to DC output efficiency of 92.2%, almost similar to the efficiency of a Tesla Powerwall [32]. The battery roundtrip efficiency from AC input to AC output is ≈0.85%. We assumed a BESS standby consumption of 0.1% of the battery inverter rating. A typical battery system is operated in a restricted SOC range due to safety reasons and to reduce aging. Consequently, the minimum state of charge (SOC_{min}) was set to 10% and the maximum SOC (SOC_{max}) to 90% of the battery storage capacity [19]. To keep the battery SOC within these constraints, the battery SOC in the first time step was set similarly as the minimum battery SOC. Hence, the battery was charged for 10% at the start of the year.

2.3.1. Real time control strategy

Charging and discharging of the battery storage, and the power flows to and from the grid for the real-time control strategy were modelled using Eqs. (5)–(9). The power flows and battery state of charge were modelled for each time step (t). The load potential (P_{pot}) depends on the difference between PV production (P_{PV}) and electricity demand (P_D), see Eq. (4).

$$P_{pot} = P_{PV} - P_D \quad (4)$$

The load potential that actually was charged or discharged is limited by the maximum AC output of the battery inverter ($P_{Binvmax}$). We assume that the maximum inverter charge power is identical to the maximum inverter discharge power, see Eq. (5).

$$P_{Bpot} = \begin{cases} P_{pot} & \text{if } |P_{pot}| < P_{Binvmax} \\ P_{Binvmax} & \text{if } |P_{pot}| \geq P_{Binvmax} \end{cases} \quad (5)$$

Next, the battery load was found using the charge (η_{charge}) and discharge ($\eta_{discharge}$) efficiencies. These efficiencies are dependent on the corresponding charge and discharge power. A charge potential was found when PV production exceeds demands, and a discharge potential was found when demand exceeds PV production. Charged or discharged energy potential (ΔE_{Bpot}) was found by multiplication of load potential with the used time interval (Δt) of 5 min, see Eq. (6).

$$\Delta E_{Bpot} = \begin{cases} P_{Bpot}\cdot\eta_{charge}\cdot\Delta t & \text{if } P_{Bpot} > 0 \\ \frac{P_{Bpot}}{\eta_{discharge}}\cdot\Delta t & \text{if } P_{Bpot} \leq 0 \end{cases} \quad (6)$$

Afterwards, the charged or discharged energy (ΔE_B) was determined. This depends on the current battery SOC ($E_{B,t}$) and is limited by the minimum battery SOC (E_{Bmin}) and maximum SOC (E_{Bmax}), see Eq. (7).

$$\Delta E_B = \begin{cases} \Delta E_{Bpot} & \text{if } E_{B,t} + \Delta E_{Bpot} \geq E_{Bmin} \\ \Delta E_{Bpot} & \text{if } E_{B,t} + \Delta E_{Bpot} \leq E_{Bmax} \\ E_{B,t} - E_{Bmin} & \text{if } E_{B,t} + \Delta E_{Bpot} < E_{Bmin} \\ E_{Bmax} - E_{B,t} & \text{if } E_{B,t} + \Delta E_{Bpot} > E_{Bmax} \end{cases} \quad (7)$$

Then, the battery state of charge ($E_{B,t+1}$) used for the next time step was found by the summation of current SOC with the charged or discharged electricity. The actual battery load (P_B) and inverter load (P_{Binv}) were calculated from the charged or discharged energy, see Eq. (8).

$$E_{B,t+1} = E_{B,t} + \Delta E_B \quad (8a)$$

$$P_B = \frac{\Delta E_B}{\Delta t} \quad (8b)$$

$$P_{Binv} = \begin{cases} \frac{P_B}{\eta_{charge}} & \text{if } P_B > 0 \\ P_B\cdot\eta_{discharge} & \text{if } P_B \leq 0 \end{cases} \quad (8c)$$

Finally, the power to the grid was determined (P_G). First, the residual power (P_R) was calculated by subtracting the electricity consumption and battery load from the PV produced power. The power flow to the grid is limited by the feed-in limit (P_{FIL}). The difference in positive power flows between the residual power and the power to the

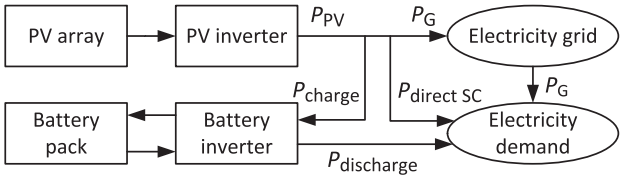

Fig. 2. Power flow diagram of an AC-coupled PV-battery system used in this study.

grid is defined as the feed-in limit loss ($P_{FILloss}$), see Eq. (9).

$$P_R = P_{PV} - P_D - P_{Binv} \tag{9a}$$

$$P_G = \begin{cases} P_R & \text{if } P_R \leqslant P_{FIL} \\ P_{FIL} & \text{if } P_R > P_{FIL} \end{cases} \tag{9b}$$

$$P_{FILloss} = \begin{cases} P_R - P_G & \text{if } P_R - P_G > 0 \\ 0 & \text{if } P_R - P_G \leqslant 0 \end{cases} \tag{9c}$$

2.3.2. Predictive control strategy

The predictive control strategy aims to reduce the curtailment losses and maintain the level of self-consumption. Therefore, it reserves a battery storage capacity to charge PV power that exceeds the feed-in limit. This reserved capacity is deployed when the actual power fed back to the grid surpasses the feed-in limit. The reserved battery state of charge was calculated with Eqs. (10) and (11).

The forecasted power that exceeds the feed-in limit (P_{FILFC}) was calculated by subtracting the forecasted electricity demand (P_{DFC}) and power feed-in limit from the forecasted PV production. This was calculated in advance for each day, thus the forecasts should be available prior to the next day. The forecasted power that was charged with the battery (P_{Bres}), depends on the battery inverter rating and charge efficiency, see Eq. (10).

$$P_{FILFC} = P_{PVFC} - P_{DFC} - P_{FIL} \tag{10a}$$

$$P_{Bres} = \begin{cases} 0 & \text{if } P_{FILFC} \leqslant 0 \\ P_{FILFC} & \text{if } 0 < P_{FILFC} < P_{Binvmax} \cdot \eta_{charge} \\ P_{Binvmax} & \text{if } P_{FILFC} \geqslant P_{Binvmax} \cdot \eta_{charge} \end{cases} \tag{10b}$$

A novel algorithm was developed to determine the reserved battery storage capacity (E_{Bres}) for each time step. The reserved battery capacity was found by the summation of reserved battery power from the start of a timeslot ($t = 1$) until the end of a timeslot ($t = end, timeslot$). The length of those timeslots varies between 5 min and 24 h, and decreases over the day. The first time step of the day (from 00:00 until 00:05) used a reserved battery capacity which was calculated for the next 24 h (from 00:00 until 00:00 the next day). The second timeslot used the battery capacity calculated for the next 23 h and 55 min (from 00:05 until 00:00 the next day). This was continued until the last timeslot of each day. Consequently, the reserved battery capacity was calculated for a declining time period for each next time step of the day. Furthermore, the reserved battery capacity was limited by the minimum and maximum battery SOC, see Eq. (11).

$$E_{Brespot} = \sum_{t=1}^{t_{end,timeslot}} P_{Brest} \cdot \Delta t \tag{11a}$$

$$E_{Bres} = \begin{cases} E_{Brespot} & \text{if } E_{Brespot} \leqslant E_{Bmax} - E_{Bmin} \\ 0 & \text{if } E_{Brespot} > E_{Bmax} - E_{Bmin} \end{cases} \tag{11b}$$

The reserved battery storage capacity was subtracted from the maximum battery capacity to find the required battery SOC. This SOC was compared with the battery SOC of the next time step that was calculated from Eq. (8). If the required SOC was lower than the battery SOC of the next time step, then the battery was only charged with PV power that exceeded the feed-in limit. Otherwise, enough battery capacity is available to charge the difference between the PV production and electricity consumption. The new potential was calculated according Eq. (12), and was used to charge the battery according Eqs. (5)–(9).

$$P_{pot} = \begin{cases} P_{PV} - P_D - P_{FIL} & \text{if } E_{Bmax} - E_{Bres} \leqslant E_{B,t+1} \\ P_{PV} - P_D & \text{if } E_{Bmax} - E_{Bres} > E_{B,t+1} \end{cases} \tag{12}$$

An example of the predictive control strategy for a residential PV-battery system is shown in Fig. 3. The predictive control strategy uses PV and demand forecasts (subplot a) to determine the surplus power (P_{top}). This predicted surplus power is used to determine a reserved battery storage capacity (E_{Bres}), shown in subplot (b). Charge of the battery storage during the day (subplot c) depends on the reserved battery capacity and the actual PV production and energy consumption.

More energy consumption is forecasted for 8th of June than what was actually consumed for that day. Hence, the reserved battery capacity is underestimated for this day and therefore the battery charges excess PV energy in the early morning hours. Consequently, the battery is fully charged at 13.00 and curtailment losses occur afterwards. The second day shows an overestimation of the demand forecast what results in a maximum battery capacity reservation for PV peak charging. The battery starts charging excess PV energy around 12:00 and the reserved battery capacity starts to decrease. The battery is fully charged around 16:30, and no curtailment losses occur on this day.

2.4. PV-battery performance indicators

The performance of control strategies with forecast methods on the PV-battery system was assessed using three annual indicators.

- Self-consumption ratio (SCR), which assess the share of direct consumed energy by the building or the battery storage system.
- Curtailment loss ratio (CLR), which indicates the share of energy lost due to a feed-in limit.
- Storage revenue ratio (SRR), which evaluates the financial gain generated by the energy that is stored in the battery relative to the revenue of a system without storage.

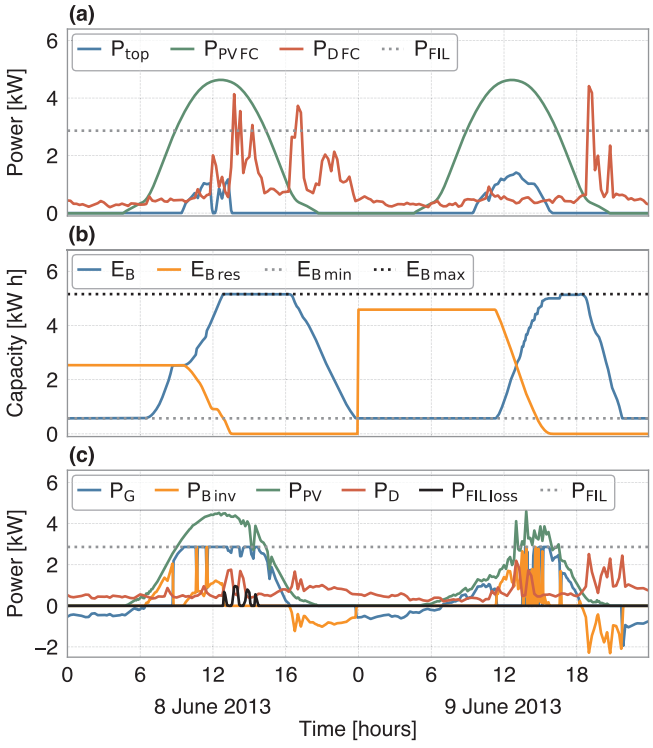

Fig. 3. Example of the predictive controls strategy operation of a residential PV-battery system for two days. The top graph (a) shows the PV forecast using PV-CS method and the demand forecast using D-PWD method. The middle graph (b) shows the reserved and actual battery state of charge. The bottom graph (c) displays the power flows to (positive) and from (negative) the electricity grid and the battery. Also the actual PV energy production, energy consumption and feed-in losses are shown. The annual consumption of this household is 5.73 MW h. Corresponding PV-battery system parameters used to this annual consumption are shown in Table 2.

Self-consumption ratio is the share of energy self-consumed (E_{SC}) from the total energy produced (E_{PV}). Self-consumed power is the power directly consumed ($P_{directSC}$) by the building added with the power used for battery charging (P_{charge}). The annual self-consumed power is aggregated from the first time step of the year (t = 1) until the last time step of the year (t_{end}), see Eq. (13).

$$P_{directSC} = \begin{cases} P_{PV} & \text{if } P_{PV} < P_D \\ P_D & \text{if } P_{PV} \geqslant P_D \end{cases} \quad (13a)$$

$$P_{charge} = \begin{cases} P_{Binv} & \text{if } P_{Binv} > 0 \\ 0 & \text{if } P_{Binv} \leqslant 0 \end{cases} \quad (13b)$$

$$E_{PV} = \sum_{t=1}^{t_{end}} P_{PV,t} \cdot \Delta t \quad (13c)$$

$$E_{SC} = \sum_{t=1}^{t_{end}} (P_{directSC,t} + P_{charge,t}) \cdot \Delta t \quad (13d)$$

$$SCR = \frac{E_{SC}}{E_{PV}} \quad (13e)$$

Curtailment loss ratio is the share of lost PV produced energy, because it cannot be fed back to the electricity grid. The CLR is found by dividing the total feed-in lost ($E_{FILloss}$) with the total produced PV energy, see Eq. (14).

$$E_{FILloss} = \sum_{t=1}^{t_{end}} P_{FILloss,t} \cdot \Delta t \quad (14a)$$

$$CLR = \frac{E_{FILloss}}{E_{PV}} \quad (14b)$$

Two annual energy flows are required to calculate the value of a PV (or PV-battery) system: the reduced electricity imported from the grid and the sold electricity to the grid. The electricity import of a building decreases because of the self-consumption. This decrease was calculated for a PV and PV-battery system using the reduced imported electricity (E_{RIE}). This is the difference between the electricity demand and the electricity imported from the grid. This imported electricity was converted to an absolute value. The sold electricity (E_{SE}) is the summation of the exported power over time, see Eq. (15).

$$E_{RIE} = \left(\sum_{t=1}^{t_{end}} P_{D,t} \cdot \Delta t \right) - \left| \left(\sum_{t|P_{G,t}<0}^{t_{end}} P_{G,t} \cdot \Delta t \right) \right| \quad (15a)$$

$$E_{SE} = \sum_{t|P_{G,t}>0}^{t_{end}} P_{G,t} \cdot \Delta t \quad (15b)$$

Storage revenue ratio indicates the annual financial value of a PV-battery system compared to a PV system without storage. It is defined as the relative change between the relative electricity revenue (RER) of these two system types. The RER of the system consists of the value of the reduced electricity imported and the sold electricity. The value of the reduced imported electricity depends on the consumption tariff (π_{cons}) and the value of the sold electricity depends on the feed-in tariff ($\pi_{feed\text{-}in}$). These tariffs depend on electricity production costs, taxes and grid network operator costs. The consumption and feed-in tariff were assumed as constant over the examined time period. Besides, we used the RER in the numerator and denominator to calculate the SRR. Consequently, we can cancel the consumption and feed-in tariff and use a new term, namely the sales to purchase ratio (SPR). This is the ratio between the feed-in tariff and the consumption tariff. As a result, we can use a single factor to include the difference between the feed-in tariff and the consumption tariff. The SPR was included in the RER, which were calculated for a PV system (RER_{PV}), and a PV-battery systems ($RER_{PV\text{-}B}$). Finally, the SRR was determined according Eq. (16).

$$SPR = \frac{\pi_{feed\text{-}in}}{\pi_{cons}} \quad (16a)$$

$$RER = E_{RIE} + (E_{SE} \cdot SPR) \quad (16b)$$

$$SRR = \frac{RER_{PV\text{-}B} - RER_{PV}}{RER_{PV}} \quad (16c)$$

The quality of the forecast methods on the PV-battery performance indicators were assessed by comparing the results from using the exact forecast (FC exact) to results from a forecast scenario (FC scenario). A forecast scenario consists of a PV forecast method and demand forecast method. The difference in performance indicator (Δ_{se}) was calculated in percentage points (%p) for the SCR, CLR and SRR, according Eq. (17).

$$\Delta_{se} = FC\,scenario - FC\,exact \quad (17)$$

3. Results

3.1. Performance of forecasting methods

The forecasted PV and energy demand patterns were compared with the actual values using nRMSE, MAPE and nMBE. Annual errors for PV patterns forecast methods are presented in Table 1. PV yield forecasting with weather prediction data (PV-WX) has the lowest nRMSE and MAPE of respectively 11.4% and 5.5%. Highest errors were found for the PV yield forecasting method that used clear-sky radiation, which is indeed a worst case considering the typically cloudy weather in the Netherlands. This method show nRMSE and MAPE that is almost two times larger than for the PV-WX method.

A higher nRMSE but an almost similar MAPE are seen for the PV-PD method compared to the PV-PW method. Thus, the PV-PD method has a larger volatility of error, but the magnitude of errors for both methods is comparable. The lower volatility of the PV-PW method is clearly caused by averaging the historical PV production data of the previous seven days. The nMBE of PV-WX is close to zero, indicating that the PV energy production is neither under or overestimated. The PV-PW and PV-WX show negative values, indicating an underestimation of PV yield. The clear-sky method has a positive error and overestimates PV yield. This overestimation is around 10 times higher nMBE error than the errors observed with the PV-PD or PV-PW.

Errors of forecasted residential and commercial demand patterns are presented using violin plots in Fig. 4. Lowest average nRMSE from residential patterns are observed for the D-PW method, specifically 7.4%. Also, this method has the smallest distribution range, from 3.2% to 11.1%. Largest errors are seen for the D-PD method, with an average of 9.5% and a maximum of 14.7%. Commercial patterns show larger differences between the forecast methods. Lowest average nRMSE is observed for D-PWD patterns, specifically 9.1%. The D-PW method shows highest errors for commercial patterns, which is in contrast with the errors seen for residential systems.

MAPEs of the demand forecast methods show similar trends as seen for nRMSE. The nMBE shows values of zero for D-PD and D-PWD methods. These methods use data of the previous day, or previous weekday. Consequently, differences between the actual and the forecasted power are averaged out to zero over the full year. The D-PW method shows a minor impact on the nMBE, with an average overestimation of electricity consumption for commercial systems.

Table 1
Annual normalized RMSE, MAPE and normalized MBE values of the PV patterns forecasting methods, for 2013.

Forecasted PV pattern	PV-PD	PV-PW	PV-WX	PV-CS
nRMSE [%]	16.98	14.98	11.35	20.64
MAPE [%]	7.79	7.82	5.51	10.51
nMBE [%]	−0.84	−0.88	−0.26	9.33

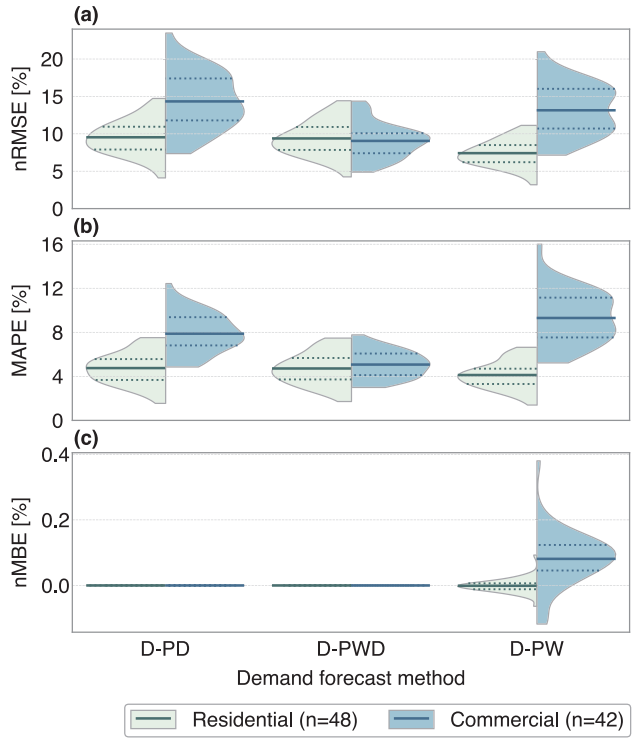

Fig. 4. Normalized RMSE (a), MAPE (b) and normalized MBE (c) of the demand forecast methods for residential patterns (left part of the violin) and commercial patterns (right part of the violin). Mean errors of the distributions are marked by solid lines, and 25% and 75% percentiles are indicated by dotted lines.

Moreover, the errors for commercial patterns are larger than for residential patterns, especially with the D-PD and D-PW method. Also, these methods have a far wider distribution range of errors than residential systems. This is related to larger differences of energy consumption between weekday and weekend days in commercial buildings than in residential buildings. Overall, residential demand forecast should include historical energy consumption of multiple days, whereas commercial demand only requires a single day.

3.2. Performance of control strategies

Real-time and predictive control strategies were assessed using performance indicators for residential and commercial PV-battery systems. The predictive control strategy has four PV forecast options and three electricity consumption forecasts options, resulting in twelve forecast options. Also, the assessment included the PC strategy using exact PV yield and exact electricity demand forecast. To sum up, one RC strategy and thirteen PC strategies were assessed.

The control strategies were assessed using similar PV-battery system parameters. All demand patterns were scaled to an annual consumption of 1 MW h, allowing us to compare patterns. Usually in the Netherlands, for each 1 MW h of annual energy consumption 1 kWp of PV is installed. This will almost fulfil the annual energy consumption. Hence, a PV system size of 1 kWp was chosen with a PV inverter of 1 kW. A battery storage size of 1 kW h for each MW h of electricity demand was chosen based on previous studies [30,33]. A battery inverter rating of 0.5 kW per kW h storage capacity was selected. This charge or discharge rate is quite common, for example with the Tesla Powerwall [32]. The feed-in limit was set to 0.5 kW per kWp installed PV capacity, based on the subsidy requirement for German PV-battery systems [4]. SRR was calculated using a sales to purchase ratio of 0.5. We assumed that the consumption tariff would be twice as high as the feed-in tariff due to the inclusion of taxation and network costs. An overview of default set of relative reference parameters is given in Table 2.

The influences of the fourteen options on SCR, CLR and SRR for the reference PV-battery systems are presented using violin plots in Fig. 5. Results from the RC strategy are shown in the most left violin plot. The second violin plot shows results from the PC strategy using exact forecasts. The remaining options present results of the PC strategy that uses all possible combinations of the PV and demand forecast methods.

3.2.1. Self-consumption ratio

Observed SCR are significantly higher in all strategies for commercial systems than for residential systems. Average residential SCR observed are between 56.6% and 57.6% under all control strategies. Commercial systems show a smaller variation in average between the control strategies, with values between 65.8% and 66.0%. Similar SCR are observed both in the RC strategy as the PC strategy, with exact forecasts. Also, PC strategy with PV pattern forecast based on weather prediction data (PV-WX) or based on the average values of last week (PV-PW) show nearly similar SCR. PC forecast using clear-sky radiation (PV-CS) show ≈0.9% point lower SCR for residential and ≈0.2% point lower SCR for commercial systems. Minor differences are observed between demand forecasting methods.

The distribution shape of commercial systems is significantly different than for residential systems. The difference between 25% and 75% percentile is ≈3.5% for residential systems and ≈2.8% for commercial systems. Yet, the total distribution range for residential patterns is ≈6% point larger than for commercial systems. A maximum SCR of 68.7% is observed for numerous commercial systems, whereas only a few residential systems show a SCR peak of 65%. This is caused by a bigger difference in time-of-use of electricity from residential buildings than from commercial buildings, see Fig. 1. The latter have relative higher energy consumption at noon, on moments with larger shares of PV produced energy. Also, residential buildings have relatively lower energy consumption in summer months when compared to commercial buildings.

3.2.2. Curtailment loss ratio

Curtailment losses are significantly lower for all PC strategies than for the RC strategy. Average CLR of residential system decreases from 5.0% for RC strategy, to 0.4% for exact forecast. The PV-CS forecast method has lowest CLR from remaining PC strategies, specifically between 0.9% and 1.2%. The PV-CS forecast overestimates PV surplus production thus more battery capacity is reserved to store these peaks. For that reason, relatively more PV energy is stored and a lower CLR is realized. Yet, a lower SCR is obtained because the battery capacity is not fully utilized to improve self-consumption. The PV-PD, PV-PW and PV-WX underestimate PV peak production. Consequently, less battery capacity is reserved and a larger share of PV peak production cannot be stored, which results in higher CLR. However, these PV forecast methods have a higher SCR because a bigger share of battery capacity is used for self-consumption.

Commercial systems show an average CLR decrease from 2.9% for RC strategy to 0.2% for PC strategy with exact forecast. Residential systems have higher curtailment losses than commercial systems under all scenarios. Commercial buildings have higher energy consumption during daytime, which are moments when PV power generation occurs. Therefore, less excess PV power is curtailed in commercial systems than

Table 2
Reference PV-battery system parameters.

Reference parameter	Value	Unit
Relative PV system size	1	$kWp_{pv}\ MW\ h_{demand}^{-1}$
Relative battery storage size	1	$kW\ h_{bess}\ MW\ h_{demand}^{-1}$
Relative battery inverter rating	0.5	$kW/kW\ h_{bess}\ MW\ h_{demand}^{-1}$
Relative feed-in limit	0.5	$kW/kWp_{pv}\ MW\ h_{demand}^{-1}$
Sales to purchase ratio	0.5	–

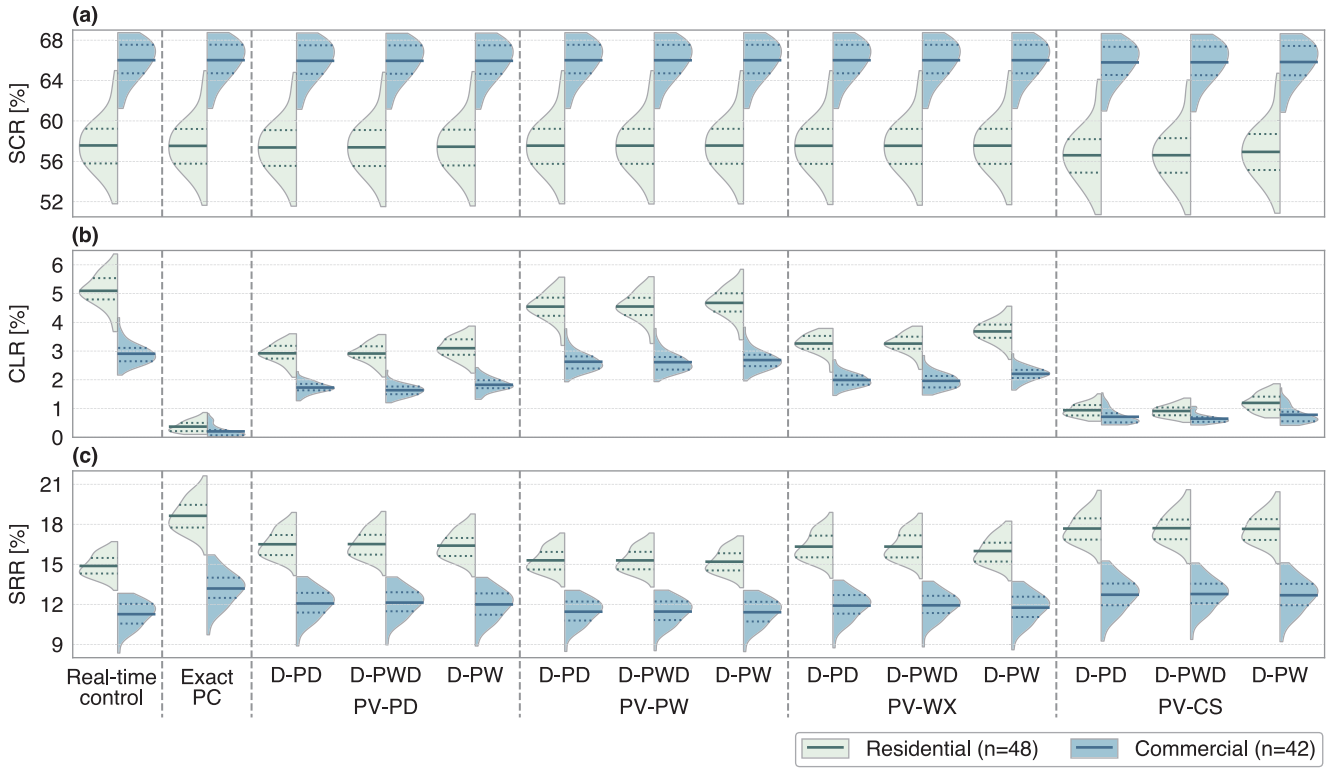

Fig. 5. Influence of control strategies on self-consumption ratio (a), curtailment loss ratio (b) and storage revenue ratio (c) for PV-battery systems using violin plots. Distributions are presented for residential systems (left) and commercial systems (right). The most left violin plots are results obtained using the real-time control strategy, while the others are obtained under the predictive control strategy. The top row of horizontal-axis labels are showing method to forecast demand, whereas the bottom row shows methods for PV energy forecasting. Used PV-battery system parameters are shown in Table 2. Mean values of the distributions are marked by solid lines, and 25% and 75% percentiles are indicated by dotted lines. Note, the results are clustered on PV forecast method for additional clarity.

in residential systems. Subsequently, the difference in CLR between the RC strategy and PC strategies is larger for residential systems. The CLR distribution range is smaller for commercial systems than residential systems and is decreasing with lower curtailment ratios. Systems with a higher SCR have a lower CLR. This explains why the CLR distribution shape of commercial systems shows the opposite shape of the distributions seen for the SCR. The reduction in CLR is limited by the reserved battery storage capacity. The influence of the reserved battery storage limits the distribution range of the residential systems.

3.2.3. Storage revenue ratio

Higher SRRs are observed for all PC strategies compared to the RC strategy. Average SRR for residential systems are increased from 14.9% for RC strategy to 18.6% for PC strategy with exact forecast. Commercial PV-battery systems show a smaller increase from 11.3% to 13.2%. This increase in storage revenues are solely caused by the reduction of the curtailment losses, which are larger for residential systems than for commercial systems. SRR distribution range for commercial system is larger than for residential systems. The distribution shape of the commercial systems is almost similar as seen with SCR, whereas residential systems show a different shape. Residential systems have higher curtailment losses, thus more value is created by reducing these losses. Consequently, the shape of the SRR distribution is influenced more by the CLR for residential systems than for commercial systems.

It is remarkable that the PC strategies that use the PV-CS forecast method show highest SRRs, but this forecast method has the largest nRMSE (see Table 1). The PV forecast method with the lowest forecast errors (PV-WX method) has lower SRRs. The PV-CS forecast method overestimates PV yield, whereas the PV-WX forecast underestimate this yield. In case of an underestimation of PV yield, not enough storage capacity is reserved and electricity is lost. In case of an overestimation of yield, sufficient storage capacity is available and no energy is lost. The underestimated yield of the PV-WX method has a lower error than the overestimated yield of the PV-CS method. Therefore a lower forecast error does not directly imply higher storage revenue.

Differences in average SRR related to the demand forecast method for PC strategies are relatively small. Furthermore, there is not a single demand forecast method that performs better for residential systems. However, the D-PWD forecast method shows the best performance for commercial systems. The difference in nRMSE between the forecasted residential demand patterns is considerably smaller than observed for commercial demand patterns, see Fig. 4. Subsequently, the influence of the demand forecast method is smaller for residential than for commercial systems.

Furthermore, the variation in PV energy production is much larger than variation in electricity consumption. Consequently, differences in nRMSE between the PV forecast methods are larger than the demand forecast methods. The difference between lowest and highest nRMSE forecast errors for the PV forecast method is 9.3% point. In contrast, this difference is 2.1% point for residential and 5.3% point for commercial demand forecasts. Thus, PV forecast methods have a larger influence than demand forecast methods.

4. Sensitivity analysis

The impact of PV-battery systems parameters on PV-battery performance indicators was assessed for six situations. The RC strategy and PC strategy with exact forecast were used to assess the absolute value of the indicator in percentage. Furthermore, four forecast scenarios were assessed to provide insight in how much influence the forecast methods have on the PV-battery system performance. These four scenarios have each another PV-forecasting method. The energy consumption forecast method with the lowest nRMSE was selected to predict electricity

demand. These are the D-PW forecast method for residential systems and the D-PWD method for commercial systems. The performance indicators of these four scenarios were compared with the performance indicators obtained with the PC strategy using exact forecasts. Differences between the exact forecast and the four scenarios (Δ_{se}) is given in percentage points (%p). An overview of these scenarios used in this sensitivity study for residential and commercial systems is given in Table 3. The evaluated system parameters were varied while other parameters were kept constant, according to reference PV-battery system values, see Table 2.

4.1. PV system size

Relative PV system size influence on the performance indicators are presented in Fig. 6. The PV system size was varied with steps of 0.01 kWp. Results from the RC strategy and PC strategy with exact forecast are presented on the left graphs. Results of differences between the four scenarios and the exact forecast are shown on the right. The locations of the line markers represent the values of reference PV-battery system parameters.

RC strategy has almost similar SCR average values as the exact PC strategy. Residential SCR decreases more rapidly than for commercial systems when PV system size increases, as shown in Fig. 6(a). The difference in SCR between residential and commercial systems increases until a relative PV system of 0.8 kWp, to a maximum of 8.8% point. Afterwards this difference reduces to 3.8% point for a 3 kWp relative PV system size. Small SCR differences are observed in the S-PW and S-WX scenarios, which states these have an almost similar performance as the exact forecast. Larger differences are seen in the S-CS scenario, with SCR of 0.9% point lower for a PV system size of 1.4 kWp. For larger PV systems, a reduction in differences is observed.

A faster increase in CLR is observed for RC strategy compared to exact PC strategy. Differences between residential and commercial CLR are larger for RC than for PC strategy, under all analysed PV system sizes. The S-CS has the largest reduction of curtailment losses, whereas the S-PW scenario has the lowest. All scenarios show a lower CLR for commercial than for residential systems. Storage revenues for PV system sizes increase until 0.4 kWp and are similar for the RC and PC strategy. For larger PV systems, SRR decreases because the battery storage system cannot store all excess PV energy. Consequently, more PV electricity is sold to the grid and electricity is lost due to the feed-in limit. This increases the revenues of a PV system without storage, and thus decreases SRR. Furthermore, larger differences in revenue between residential and commercial systems are observed. The S-CS scenario shows the best performance, with a SRR difference of ≈1% for all analysed PV system sizes.

4.2. Battery storage capacity

The impacts of relative battery storage capacities with a 0.01 kW h step size are shown in Fig. 7. SCR increases related to larger battery capacities, and is larger for residential than for commercial systems. Residential systems increase from 32.2% to 75.1% and commercial systems from 44.0% to 79.0%. The battery storage capacity has a minor effect on the difference in SCR between the RC and PC strategy. The S-CS scenario overestimates PV yield production, therefore more storage capacity is reserved than is needed to store the excess PV power. So, a large difference is observed between the exact and the S-CS scenario, which peaks at a storage capacity of around 0.5 kW h. The share of reserved battery that is overestimated from the total battery capacity reduces with larger battery storage capacities. Consequently, the difference with the exact forecast is reduced and reaches similar values as the other three forecast strategies (at 2.5 kW h).

With an increase in battery size, curtailment losses are faster decreasing for exact PC strategy compared to RC strategy. CLR decreases with the exact PC strategy from ≈5.8% to 0.1% for residential systems and from ≈3.3% to 0.08% for commercial systems. This means that larger battery storage capacities are required to completely eliminate curtailment losses. Large Δ_{se} are shown for the S-PW and small Δ_{se} for the S-CS scenario.

SRRs are higher for residential than for commercial systems, and higher for exact PC strategy than for RC strategy. Storage revenues show an almost linear increase until a storage capacity of ≈0.5 kW h. Highest SRRs are reached at capacity of 2.75 kW h, specifically 25.0% for residential systems. Commercial systems reach a maximum SRR of 16.7% at a storage capacity of 2.4 kW h. A small drop in SRR is observed for larger storage capacities, caused by higher share of charging and discharging losses. For this reason, larger battery sizes are not recommended. The S-CS scenario has the largest revenue of all used forecast scenarios, which is similar as observed for the PV system size sensitivity analysis.

4.3. Battery inverter rating

The impact of relative battery inverter rating, for steps of 0.0025 kW, is presented in Fig. 8. Comparable SCR for the RC strategy as for the exact PC strategy are shown. SCR is rapidly increased until a battery inverter rating of ≈0.1 kW, and converges to a maximum of 57.9% for residential and ≈66.3% for commercial systems.

An interesting observation for the RC strategy can be made concerning the relation between battery inverter rating and curtailment loss. CLR decreases until an inverter rating of 0.12 kW, but show an increase for larger capacities. A lower inverter rating limits the charge rate of a battery, i.e. the battery is charged slower. As a result, additional battery capacity becomes available to charge PV peak energy and therefore reduces curtailment loss. This limited battery charging disappears with ratings > 0.6 kW because no change in curtailment loss is observed for these capacities.

SRR of residential and commercial systems are increased using the RC strategy until a rating of 0.19 kW. Using the PC strategy, this increase is observed until 0.4 kW for residential and 0.33 kW for commercial systems. Larger inverters have a higher share of energy loss due to the battery and inverter efficiencies, which results in lower revenues. For this reason, battery inverters with ratings > 0.4 kW per kW h of storage capacity are not recommended.

4.4. Feed-in limit

Influence of the relative used feed-in limit with steps of 0.025 kW, are presented in Fig. 9. The RC strategy does not affect the timing of battery charging or discharging, thus is not affected by the feed-in limit. With the exact PC strategy, battery capacity is reserved to store PV energy which exceeds the feed-in limit. Consequently, under a restricted feed-in limit, less energy can be stored and discharged on later moments. This results in a small reduction of SCR, especially visible for residential systems.

PC strategies show a decrease of SCR until a certain FIL, thereafter followed with an increase in SCR. This is especially visible for scenarios where there is an overestimation of the PV energy production, namely the S-CS scenario. A more strict limitation (towards 0 kW) requires a higher share of reserved battery capacity to store excess PV. Hence, relatively less storage capacity is available to store direct excess PV

Table 3
Overview of forecast scenarios for residential and commercial systems, assessed in the sensitivity analysis.

Scenario name	S-PD	S-PW	S-WX	S-CS
PV yield forecast	PV-PD	PV-PW	PV-WX	PV-CS
Residential demand forecast	D-PW	D-PW	D-PW	D-PW
Commercial demand forecast	D-PWD	D-PWD	D-PWD	D-PWD

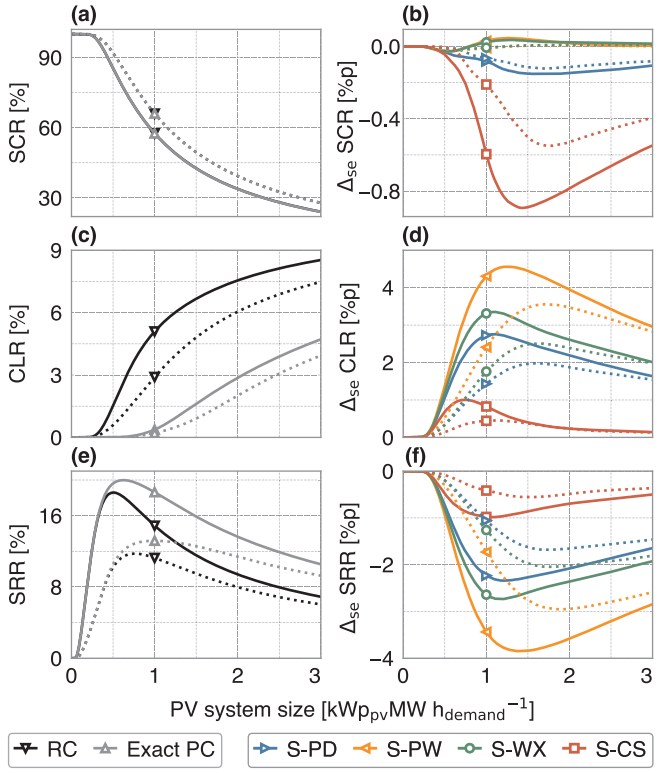

Fig. 6. Influence of relative PV system size on SCR (a), CLR (c) and SRR (e) for the real-time control (RC) and the predictive control with exact forecast (Exact PC). Difference between forecast scenario and exact forecast (Δ_{se}) in SCR (b), CLR (d) and SRR (f) are shown for four scenarios in percentage points [%p]. The solid lines show the average value of residential systems and the dotted lines show averages of commercial systems. An overview of the scenarios is given in Table 3. Remaining system parameters are given in Table 2. The markers indicate the reference PV-battery system values.

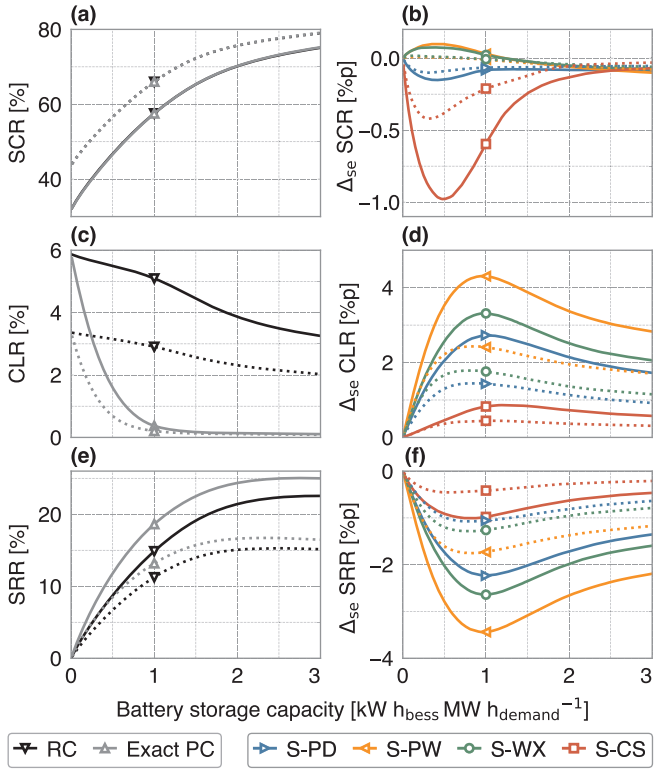

Fig. 7. Influence of relative battery system capacity on SCR (a), CLR (c) and SRR (e) for the RC and PC with exact forecast, and difference in SCR (b), CLR (d) and SRR (f) of the scenarios minus the exact forecast. The solid lines show the average value of residential systems and the dotted lines show averages of commercial systems. Reference system values are indicated by the markers.

energy. For more relaxed limitations (towards 1 kW), less PV peak power must be curtailed. Subsequently, a lower amount of storage capacity is reserved for excess PV peak power, and more storage capacity is available for self-consumption.

Using the RC strategy, curtailment losses are eliminated at a FIL of ≈0.85 kW. The PC strategy completely removes these losses at a FIL of ≈0.7 kW. The FIL shows a large sensitivity of the used forecast scenario. For residential systems, the S-WX scenario has higher CLR reduction compared to the S-PD scenario, with feed in limits < 0.4 kW. The opposite is seen for more relaxed FILs. This shows that the weather forecast method underestimate the PV peaks (> 0.4 kW) compared to the PV-PD method. This could be caused by the weather forecast time step of 3 h used in the PV-WX forecast method. Therefore, PV peaks are averaged out, which is also shown for the PV-PW method. Subsequently, battery capacity reservations for these higher peaks are lower, and curtailment losses are higher.

When no PV energy can be fed back to the grid, similar SRRs are shown for RC as for PC strategy. Corresponding SRR are 69.2% for residential and 43.4% for commercial systems. Benefits of PC strategy over RC strategy increase until a FIL of 0.2 kW for both residential and commercial systems. With these feed-in limits, SRR are 8.2% point higher for residential systems and 6.0% point higher for commercial systems, as shown in Fig. 9(e). For more relaxed limitations (towards 1 kW), differences between the RC and PC strategy disappear. Storage revenues with a FIL of 1 kW depend only on the increased PV self-consumption. The S-CS scenario shows the highest SRR, whereas lowest SRR are observed in the S-PW scenario.

4.5. Sales to purchase ratio

Sales to purchase ratio solely affects storage revenues, therefore only influences on SRR are presented in Fig. 10. SPR was varied with steps of 0.0025 between 0 and 1. Thus, we assumed only electricity feed-in tariffs that are lower than the electricity consumption tariff.

With an SPR of zero, electricity fed back to the grid has no financial value, which means that reducing curtailment loss has no financial benefit. Consequently similar SRRs are seen for RC and PC strategy, with significantly larger values for residential (70.3%) than for commercial system (33.8%). An increase in SPR results in an increased value of sold electricity and thus a decrease in SRR. It is essential to note that the RC strategy drops below zero, at a SPR of 0.86. For this SPR, the value of added self-consumed energy due to energy storage is not sufficient enough to compensate for charge and discharge losses of the BESS. Thus, the battery storage system will have no added revenue for these conditions. Nevertheless, the exact PC strategy has positive SRR for all analysed sales to purchase ratios. In this scenario, PV produced electricity that would be lost due to feed-in limitation is stored and later used which increases the SRR to a positive value.

A large influence of the PV forecast scenario on SRR of the PV-battery system is seen. A reduction of SPR results in a decrease of the value of sold electricity. Subsequently, the value of self-consumption increases, whereas the value of reducing curtailment loss decreases. The opposite effect occurs for relatively larger SPR. The S-WX scenario shows highest SCR, whereas the S-CS scenario has lowest CLR. Consequently, residential systems with a SPR < 0.13 have highest SRR in the S-WX scenario. The S-PD scenario shows the largest SRR for a SPR 0.13 and 0.18, whereas for larger SPR the S-CS scenario has the highest revenue. Commercial systems have a turning point between the S-WX and the S-CS at a SPR of 0.11, which is lower than for residential systems.

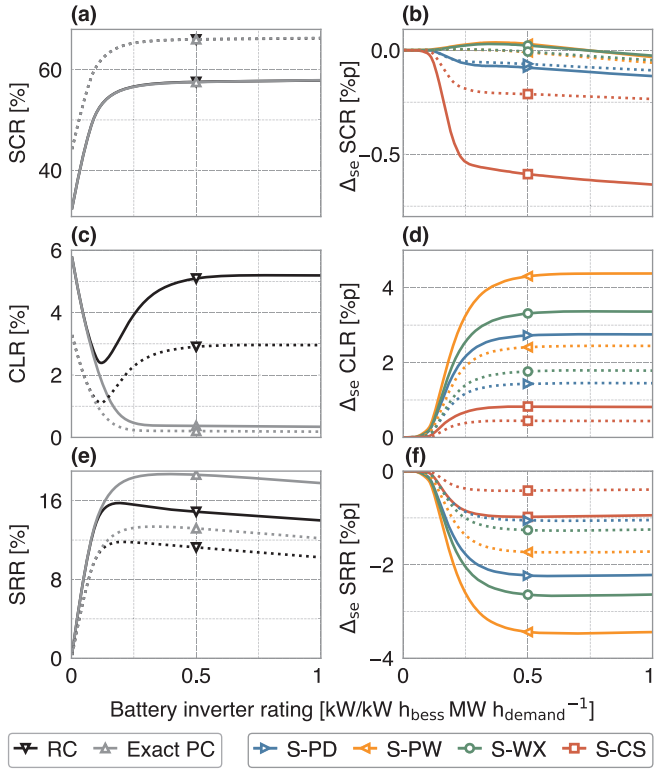

Fig. 8. Influence of battery inverter rating on SCR (a), CLR (c) and SRR (e) for the RC and PC with exact forecast, and difference in SCR (b), CLR (d) and SRR (f) of scenarios minus exact forecast. Residential systems are indicated by solid lines and commercial systems are indicated by dotted lines. Reference system values are indicated by the markers.

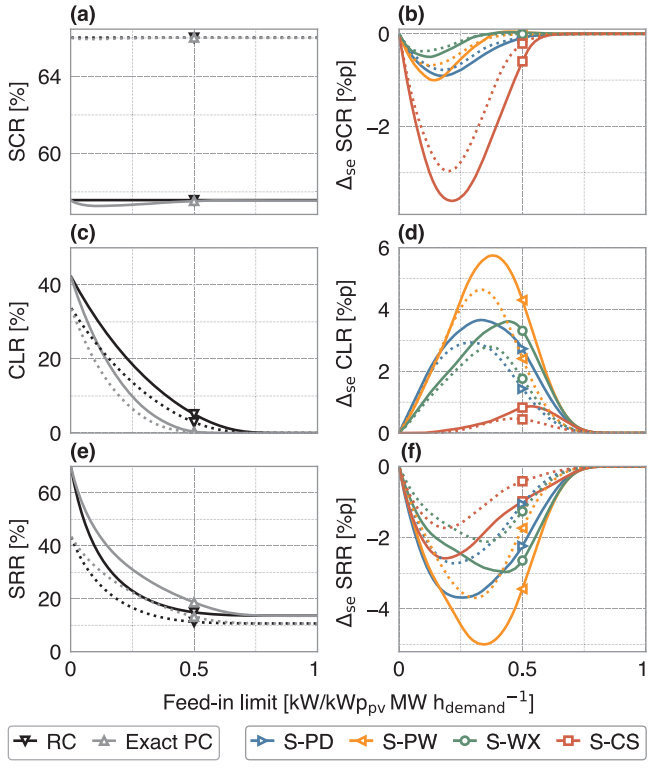

Fig. 9. Influence of the relative feed-in limit on SCR (a), CLR (c) and SRR (e) for the RC and PC with exact forecast, and difference in SCR (b), CLR (d) and SRR (f) of scenarios minus exact forecast. Residential systems are indicated by solid lines and commercial systems are indicated by dotted lines. Reference system values are indicated by the markers.

4.6. Impact of system degradation

A commonly heard concern regarding PV-battery systems is the influence of degradation on the performance of these systems. Therefore, we assessed the influence of PV systems and BESS degradation for a period of 25 years. A relative long lifetime was investigated to assess the possible impact of systems that keep operating even when economic lifetime has passed. We assumed a PV systems degradation value of 0.5% per year [34]. The real-time PV yield pattern and forecasted PV yield patterns were annually reduced with 0.5%. BESS degradation was modelled for a lifetime of 5000 full cycle equivalents and a calendric lifetime of 15 years [35]. 80% of the initial battery capacity is reached after these cycles, or after this lifetime. Rainflow counting method was used to count the number of battery cycles and depth of discharge for each cycle, for each year of data [36]. These numbers were converted to the number of full equivalent cycles, based on degradation parameters from previous studies [35,37]. Annual PV yield and battery storage capacity degradation were subtracted from the previous year to find the capacity values for the next year.

The impact of PV system and BESS degradation on the performance indicators are presented in Fig. 11. PV system degradation reduces PV electricity production over time, which increases PV self-consumption. Battery degradation reduces battery storage capacity and decreases self-consumption. Residential systems show a reduction from 57.6% to 55.6%, with an average reduction of 0.08% point per year. Commercial systems show a slight reduction in SCR until year 18, followed with an increase in SCR. Residential systems utilize the battery more than commercial systems. Therefore the impact of battery degradation is larger than the impact of PV system degradation on self-consumption. This results in a SCR reduction for each year. The battery degradation is less severe for commercial system. After 18 years, a larger effect on the SCR is observed from the PV system degradation than from the battery storage capacity degradation.

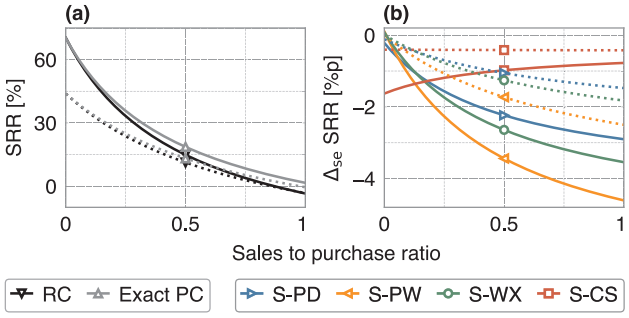

Fig. 10. Influence of the sales to purchase ratio on SRR (a) for the RC and PC with exact forecast, and difference in SRR (b) of scenarios minus exact forecast. Residential systems are indicated by solid lines and commercial systems are indicated by dotted lines. Reference system values are indicated by the markers.

The difference between the exact strategy and the forecasting strategies are reduced over the systems lifetime. Larger reduction is shown for the S-CS strategy, caused by a larger reduction in forecasted PV electricity yield. Subsequently, less battery storage capacity is reserved to decrease feed-in losses and more capacity is available to increase self-consumption.

A reduction in PV yield results in lower curtailment losses. CLR show a steeper decrease over time in the RC strategy compared to the exact PC strategy. The forecast scenarios show a reduction over time caused by less PV production, except for the S-CS strategy. This strategy does not show a decrease because the PV yield production is overestimated and therefore the reserved storage capacity was already sufficient to have a low CLR.

A larger reduction of storage revenue over time is seen for

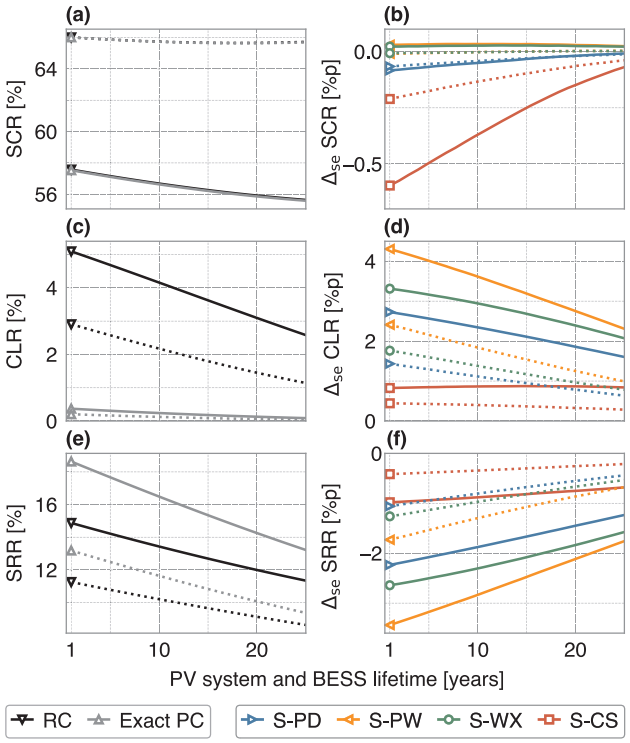

Fig. 11. Influence of PV system and BESS degradation on the SCR (a), CLR (c) and SRR (e) for the RC and PC with exact forecast, and difference in SCR (b), CLR (d) and SRR (f) of scenarios minus exact forecast. Residential systems are indicated by solid lines and commercial systems are indicated by dotted lines. Reference system values are indicated by the markers.

residential systems than for commercial systems. Residential systems show a reduction in SRR of 0.21% point per year in the exact PC strategy and of 0.14% point per year in the RC strategy. This results in a significant loss of storage revenues over the system lifetime of respectively 14.1% and 17.9% in the PC and the RC strategy. Commercial systems have a lower SRR reduction of 10.5% and 12.5% in the PC and the RC strategy. The SRR difference between the exact forecast and the forecast scenarios decreases over time for all scenarios.

4.7. Multiple system parameter variation

The influences of simultaneous variation of multiple system parameters on the storage revenue rates have been assessed. The PC strategy with exact forecast was used to examine the potential of this control algorithm on the SRRs. The average SRRs for residential systems are shown for 12 scenarios in Fig. 12. Battery storage capacity (horizontal axis, step of 0.01 kW h) and sales to purchase ratio (vertical axis, steps of 0.025) are shown on each of the subplots. Four feed-in limitations (0, 0.25, 0.5, 0.75 kW) and three PV system sizes (0.5, 1 and 1.5 kWp) were assessed. The influence of battery inverter rating which are commonly used (> 0.5 kW) on the storage revenue ratio is minor (see Fig. 8). Hence, this parameter was kept constant at 0.5 kW per kW h of storage capacity.

The electricity cannot be sold back to the grid under a FIL of zero. Consequently, the sales to purchase ratio does not influence SRR and an increase in battery storage capacity results in a non-linear growth of storage revenues. Similar storage revenues rates are seen for the three PV system sizes with relative small battery storage capacities (< 0.5 kW). Larger differences in SRRs are observed with battery capacities of 3 kW h. These are 80.0%, 110.9% and 117.9% for respectively 0.5, 1 and 1.5 kWp PV size. The difference in SRR between a PV system size of 0.5 kWp and 1 kWp is larger than between 1 and 1.5 kWp. Larger PV systems produce more surplus of electricity that could be stored in the battery. Yet, the electricity consumption is similar for all PV system sizes. Therefore fewer moments occur that the battery will be discharged for these larger PV systems, which results in a lower increase of SRRs.

Electricity is lost in every moment that a battery is charged and discharged. This reduces storage revenue rates, which eventually become negative. For smaller battery capacities, the value added due to reduced curtailment losses is higher than the value lost caused by battery charge and discharge losses. Hence an increase is observed in SRR. A peak in SRR is observed for a certain battery capacity followed by a decrease for larger battery capacities. This peak in the contour lines disappears with a lower SPR, which increase the value of self-consumption.

Only positive SRRs are observed under the FIL of 0.25, whereas under larger other FIL (0.5 & 0.75) negative SRRs are shown. In addition, a FIL of 0.5 shows that the area of negative values decreases for larger PV system sizes. These larger systems produce more PV electricity that exceeds the feed-in limit, which eventually increase revenues of a BESS. Less battery capacity is reserved for a FIL of 0.75 kW, therefore more capacity is available to increase self-consumption. However, for high SPRs (> 0.85), the added value of self-consumption is negative due to battery charge and discharge losses. Consequently, more electricity is lost by increasing self-consumption than lost by a feed-in limit. This explains why the difference in negative areas of the PV system sizes is much smaller for a FIL of 0.75 than for a FIL of 0.5.

5. Discussion

This research developed and assessed four methods for PV forecasting and three methods for demand forecasting. These forecasts were used in a predictive control strategy to increase PV self-consumption and to reduce curtailment losses. We assessed the impact of these forecast methods using a PC strategy on the performance of PV-battery systems.

We found significant impact of the system design parameters on the performance indicators. Increasing the PV system size lowers self-consumption rates and increases curtailment loss. Larger battery capacities converges the storage revenues towards a maximum, followed by a decrease of revenue. Battery inverter ratings of 0.6 kW for each kW h of storage are sufficient for PV peak power storage, especially with a feed-in limit of 0.5 kW/kWp. A strong decrease in performance indicators is observed for smaller inverter capacities. The ratio between the feed-in tariff and the consumption tariff strongly influence the value of the self-consumed and avoided curtailed energy. Battery degradation substantially reduces the storage revenues over the lifetime of the battery system and should therefore be always included in economic calculations. Overall, these results showed that the system performance heavily depends on the chosen PV-battery design parameters, demand pattern and electricity tariff.

5.1. Comparison with previous studies

Forecast errors of predicted PV yield and electricity demand are in line with errors found in previous studies. Artificial neural networks were used to predict hourly PV yield and energy consumption for a German household. PV forecast errors with a nRMSE of 9.5% and electricity consumption errors of nRMSE of 9.3% were found in this study [21]. A nonlinear autoregressive with exogenous input model was tested which used weather and measurements of neighbouring PV systems to create PV yield forecasts, and revealed nRMSE between 9% and 25% [38]. Another research forecast residential load found MAPE errors of ≈1% lower using a multiple linear regression forecast than using the 7 days average, which is a similar method as used in this study [39]. Deep neural network based load forecasting models were used to predict commercial load and found average MAPE of 8.8% [40]. Our study showed lowest annual nRMSE of 11.4% for PV yield forecast and

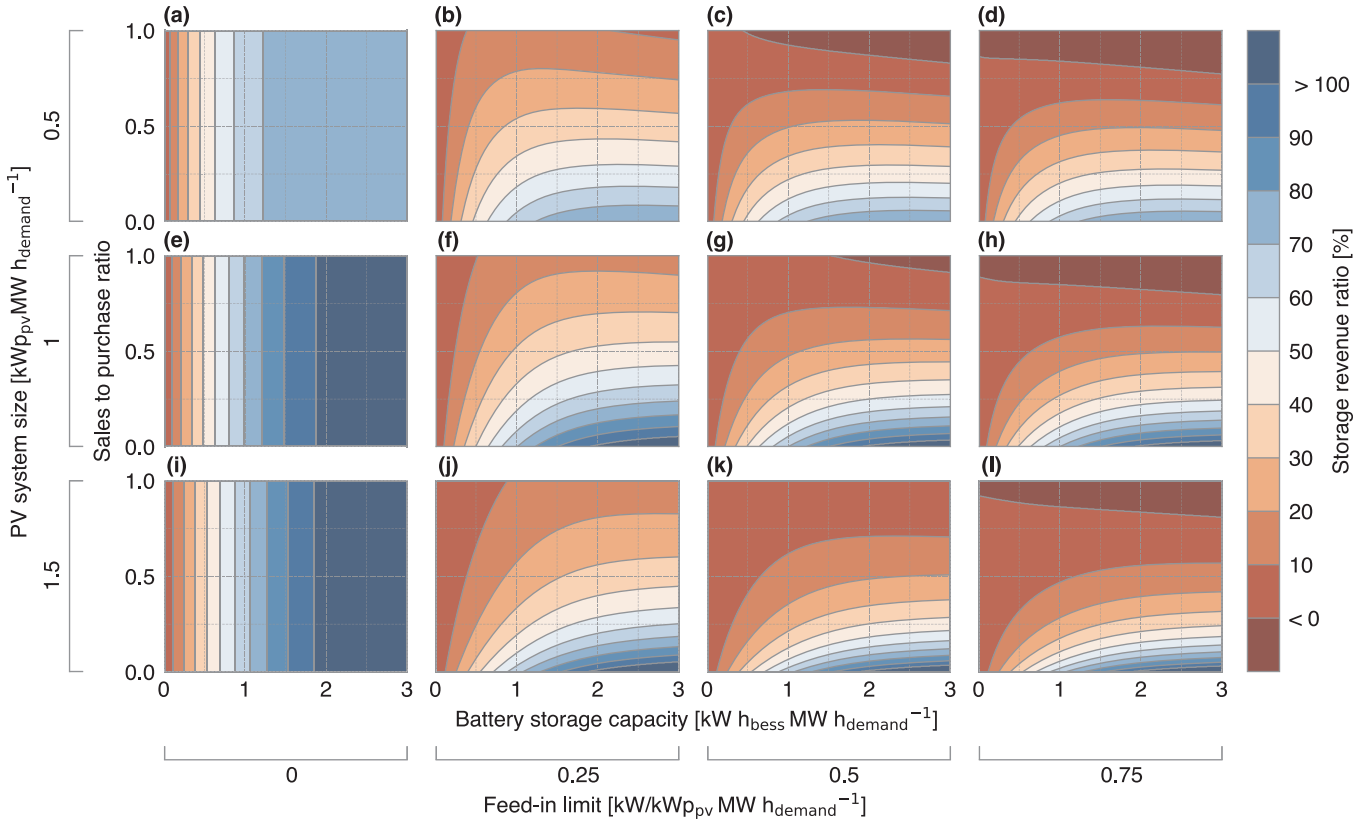

Fig. 12. Influence of the battery storage capacity (horizontal axis) and the sales to purchase ratio (vertical axis) on the average storage revenue ratio (colours). The storage revenues were assessed using the PC strategy with the exact forecast for residential systems. Four feed-in limitations (0, 0.25, 0.5, 0.75 kW) and three PV system sizes (0.5, 1 and 1.5 kWp) are shown in the subplots. Similar feed-in limits are shown in columns and PV system sizes in rows. For example, the subplot (a), (e) & (i) show the values for a feed-in limit of 0 kW, and the subplot (a), (b), (c) & (d) show values for a PV system size of 0.5 kWp. The battery inverter ratings were kept constant at 0.5 kW per kW h of battery storage capacity. (For interpretation of the references to colour in this figure legend, the reader is referred to the web version of this article.)

7.4% as the average for residential demand. Our forecast errors are in line with the more sophisticated models presented in previous studies.

Performance of the PV-battery systems showed similarities with earlier studies. The RC control strategy shows that residential self-consumption rates are ranging between 51.8% and 65.0%, which is in line with values found in previous studies [10,41]. Similar PV-battery performance is shown for using averaged energy demand and PV energy production from the previous week [16]. No comparable study was found for commercial systems that were mainly modelled for office buildings. The clear-sky forecast method shows comparable reduction of curtailment loss to a study which used this method with demand patterns from Switzerland [11]. However, this study presents a smaller difference in self-consumption between the RC strategy and PC strategy with exact forecast. This is caused by the used battery capacity reservation algorithm, which uses the demand forecast as input to determine the required battery capacity reservation.

Studies concluded that an overestimation of forecasted PV yield production results in lower self-consumption rates but also lower curtailment losses [10,14]. No direct comparison could be made on specific storage revenues because this method was not used in previous research. Still, the convergence to a maximum of storage revenue under an increase in battery size was shown before [11,13].

5.2. Input data

The energy consumption of residential and commercial buildings was measured using an interval of 15 min. Also, the real-time PV pattern was modelled using radiation data of a 10 min interval. Both patterns were resampled to 5 min interval to match the time step interval. However, actual patterns have a higher fluctuation of power than the used pattern. For example, extreme variation of PV system power output could be expected with passing clouds. Both PV production and demand patterns are more flattened compared to actual patterns. This changes the overlap of the patterns, and therefore affects the self-consumption and the operation of battery control strategies. Previous studies examined the effect of time resolution on the performance of PV-battery systems. Relative errors below 6% were found for using 15 min data for self-consumption calculations [42]. Curtailment loss ratio was 2.8% point lower with 15 min data, compared to using 5 s data [11]. Consequently, higher storage revenue ratios could be obtained than presented in this study. Therefore, we recommend assessing the proposed forecast methods with data of a higher time resolution.

The obtained weather prediction data has a time resolution of 3 h, but using data with smaller time resolutions could improve this forecast. The PV peak production forecast on clear-sky days will be better predicted. Nevertheless, day-ahead forecasting of moving clouds and thus the right timing of PV peak production is very difficult. Especially, because the Netherlands has a cloudy climate. Further research on the impact of smaller time resolution of weather prediction data on performance of PV-battery systems is recommended.

The average specific yield in the Netherlands is 875 kW h/kWp, which is lower than the specific yield used in our study [43]. The optimal orientation for maximizing PV energy production was chosen to model PV yield, whereas for actual PV systems the orientation of a building influences the PV module orientation. This reduces the PV yield which increases self-consumption and lowers curtailment losses. Both effects cause lower storage revenues. Hence, it is recommended using real PV pattern measurements with different orientations for

future studies.

5.3. Future trends

Other options to improve PV energy integration in the urban energy systems are currently rapidly developed. These options could compete with local residential and commercial energy storage. Especially, community energy storage could be more economically feasible for reducing low voltage grid impact and increasing locally consumed PV energy [44]. However, a detailed layout of the low-voltage grid is required to accurate include grid-losses. Nevertheless, further research concerning technical and economic comparison of local and community energy storage systems is recommended. Also, the comparison of forecast methods for local and community storage systems could be of interest.

Rescheduling residential and commercial appliances could shift energy consumption to moments with relatively high PV energy generation, for example using dynamic tariffs [45]. However, these options demonstrate relative low improvement in PV self-consumption, therefore having low economic potential [46,47]. Nevertheless, the current increase of electrical vehicle deployment increases the electricity demand within urban areas. This opens new opportunities to increase PV-self-consumption by control strategies for electrical vehicle charging [48]. Also, control strategies that combine thermal and electric storage are investigated to improve residential self-consumption [49].

Battery energy storage systems can provide services for different electricity markets. For example, provision of frequency control to balance and maintain grid frequency. Combining multiple revenue streams for energy storage improves the revenues for battery storage systems [50]. Control strategies that combine revenue streams depend on the associated energy markets and policies. Assessment of these strategies is recommended for future research.

Reducing power flow to the grid lowers grid-investment costs, especially for cables and transformers. A reimbursement to the PV-battery system owner could be provided for this service, resulting in increased storage revenues. Finally, this study used no time-dependent electricity tariffs and feed-in limits. Time-of-use electricity tariffs and dynamic feed-in limits could increase the value of PV-battery systems. Battery energy storage revenues might differ significantly when time-of-use tariffs will be used for both consumption and feed-in tariffs. These tariffs are commonly used, especially for large commercial buildings. It is expected that the variability in electricity prices will increase with larger share of fluctuating renewable electricity generation capacity. Therefore, trading on electricity markets could be possible with batteries, and increase the economic value of the battery energy storage systems. However, this requires knowledge about the structure and decision models of time-of-use tariffs and dynamic feed-in limits. Forecast methods should be developed and assessed that optimize storage revenue for flexible tariffs and dynamic tariffs. Research in those areas is therefore highly recommended.

5.4. Implementation considerations

The implementation of forecast algorithms in battery energy management systems requires some adjustments. First, measurements of historical consumption data are required, which could be obtained from smart energy meters. These electricity meters are currently deployed within the Netherlands and have an option to send measured data to other devices. Historical PV production could be obtained from PV inverters. Predicted weather forecast data requires an internet connection. Clear-sky irradiance data can be calculated internally using the battery energy management system. Also the forecast strategies could be installed on these management systems.

The developed methods could be used in other European countries. These countries have different PV yield and demand patterns compared to the Netherlands. This will influence the accuracy of the forecast methods and the PV-battery performance indicators. For example, more PV peak power is produced in Southern European countries compared to the Netherlands. Therefore, relatively more PV peak power can be stored and therefore the reduction in curtailment losses is larger. Consequently, revenues of battery storage are expected to be higher.

6. Conclusion

This study assessed four PV yield pattern forecast methods and three demand patterns forecast methods. These forecasts were used in a predictive control strategy to improve self-consumption, reduce curtailment loss and increase revenues of PV-battery systems. We modelled performance of 48 residential and 42 commercial PV-battery systems, using different combinations of forecast methods.

We found that the PV production patterns with predicted weather data have lowest errors. Energy consumption of residential buildings should be forecasted with using average energy consumption of the previous seven days. Forecast for commercial systems should use measured historical demand from the previous weekday. Weather forecasts are not required to increase self-consumption rate, since forecasts using historical PV production data show similar performance. Consequently, external data is not required to optimize PV self-consumption.

Predictive control strategies have higher storage revenues that real-time control. Storage revenues are larger for residential systems than for commercial systems and mainly depend on the value of self-consumed energy and reduced curtailed energy. Higher storage revenues are observed for stricter feed-in limitations. Consequently, a dynamic feed-in limitation could potentially increase storage revenues. The sales to purchase ratio strongly impacts revenues obtained for each used control strategy and forecast method.

To conclude, predictive control strategies are capable to improve self-consumption, as well as reduce curtailment losses. The performance of the battery control strategy depends on PV-battery system design parameters as well as system boundaries conditions, especially feed-in limit and sales to purchase ratio. Hence, it is recommended to customize the battery control strategy based on these conditions.

Acknowledgements

This work is part of the research programme Transitioning to a More Sustainable Energy System (Grant No. 022.004.023), which is financed by the Netherlands Organisation for Scientific Research (NWO). We are grateful to Hubert Spruijt of Senfal, Liander N.V. and the Royal Netherlands Meteorological Institute for providing data.

References

[1] Louwen A, van Sark W, Faaij A, Schropp R. Re-assessment of net energy production and greenhouse gas emissions avoidance after 40 years of photovoltaics development. Nat Commun 2016;7:13728 EP–, articl. http://dx.doi.org/10.1038/ncomms13728.
[2] International Energy Agency Photovoltaic Power Systems Programme (IEA PVPS). 2015 Snapshot of global photovoltaic markets. Tech rep; 2016.
[3] European Commission. Best practices on renewable energy self-consumption. Tech rep. European Commission, Brussels; 2015.
[4] KfW. KfW-Programm Erneuerbare Energien Speicher; 2017. URL < https://www.kfw.de/Download-Center/F%C3%B6rderprogramme-(Inlandsf%C3%B6rderung)/PDF-Dokumente/6000002700_M_275_Speicher.pdf > .
[5] Antonanzas J, Osorio N, Escobar R, Urraca R, de Pison FM, Antonanzas-Torres F. Review of photovoltaic power forecasting. Sol Energy 2016;136:78–111. http://dx.doi.org/10.1016/j.solener.2016.06.069.
[6] Elsinga B, van Sark WG. Short-term peer-to-peer solar forecasting in a network of photovoltaic systems. Appl Energy 2017;206(Suppl C):1464–83. http://dx.doi.org/10.1016/j.apenergy.2017.09.115.
[7] Khan AR, Mahmood A, Safdar A, Khan ZA, Khan NA, forecasting Load. dynamic pricing and DSM in smart grid: a review. Renew Sustain Energy Rev 2016;54:1311–22. http://dx.doi.org/10.1016/j.rser.2015.10.117.
[8] Torriti J. A review of time use models of residential electricity demand. Renew Sustain Energy Rev 2014;37:265–72. http://dx.doi.org/10.1016/j.rser.2014.05.034.

[9] Resch Matthias, Bühler Jochen, Klausen Mira, Sumper Andreas. Impact of operation strategies of large scale battery systems on distribution grid planning in Germany. Renew Sustain Energy Rev 2017;74:1042–63. http://dx.doi.org/10.1016/j.rser.2017.02.075.

[10] Moshövel J, Kairies KP, Magnor D, Leuthold M, Bost M, Gährs S, et al. Analysis of the maximal possible grid relief from PV-peak-power impacts by using storage systems for increased self-consumption. Appl Energy 2015;137:567–75. http://dx.doi.org/10.1016/j.apenergy.2014.07.021.

[11] Riesen Y, Ballif C, Wyrsch N. Control algorithm for a residential photovoltaic system with storage. Appl Energy 2017;202:78–87. http://dx.doi.org/10.1016/j.apenergy.2017.05.016.

[12] Riffonneau Y, Bacha S, Barruel F, Ploix S. Optimal power flow management for grid connected PV systems with batteries. IEEE Trans Sustain Energy 2011;2(3):309–20. http://dx.doi.org/10.1109/TSTE.2011.2114901.

[13] Williams C, Binder J, Danzer M, Sehnke F, Felder M. Battery charge control schemes for increased grid compatibility of decentralized PV systems. In: 28st European photovoltaic solar energy conference and exhibition, WIP-renewable energies, Munich, Germany; 2013. p. 3751–6. http://dx.doi.org/10.4229/28thEUPVSEC2013-5CO.7.6.

[14] Bergner J, Weniger J, Tjarko T, Quaschning V. Feed-in power limitation of grid-connected PV battery systems with autonomous forecast-based operation strategies. In: 29st European photovoltaic solar energy conference and exhibition, WIP-renewable energies, Munich, Germany; 2014. p. 2363–70. http://dx.doi.org/10.4229/EUPVSEC20142014-5CO.15.1.

[15] Zeh A, Witzmann R. Operational strategies for battery storage systems in low-voltage distribution grids to limit the feed-in power of roof-mounted solar power systems. Energy Proc 2014;46:114–23. http://dx.doi.org/10.1016/j.egypro.2014.01.164.

[16] Waffenschmidt E. Dimensioning of decentralized photovoltaic storages with limited feed-in power and their impact on the distribution grid. Energy Proc 2014;46:88–97. http://dx.doi.org/10.1016/j.egypro.2014.01.161. 8th International Renewable Energy Storage Conference and Exhibition (IRES 2013).

[17] AlSkaif T, Schram W, Litjens G, van Sark W. Smart charging of community storage units using markov chains. In: 2017 IEEE PES innovative smart grid technologies conference Europe (ISGT-Europe); 2017. p. 1–6. http://dx.doi.org/10.1109/ISGTEurope.2017.8260177.

[18] Ranaweera I, Midtgård O-M. Optimization of operational cost for a grid-supporting PV system with battery storage. Renew Energy 2016;88:262–72. http://dx.doi.org/10.1016/j.renene.2015.11.044.

[19] Li J, Danzer MA. Optimal charge control strategies for stationary photovoltaic battery systems. J Power Sources 2014;258:365–73. http://dx.doi.org/10.1016/j.jpowsour.2014.02.066.

[20] Angenendt G, Zurmühlen S, Mir-Montazeri R, Magnor D, Sauer DU. Enhancing battery lifetime in PV battery home storage system using forecast based operating strategies. Energy Proc 2016;99:80–8. http://dx.doi.org/10.1016/j.egypro.2016.10.100.

[21] Klingler A-L, Teichtmann L. Impacts of a forecast-based operation strategy for grid-connected PV storage systems on profitability and the energy system. Sol Energy 2017;158:861–8. http://dx.doi.org/10.1016/j.solener.2017.10.052.

[22] Andrews RW, Stein JS, Hansen C, Riley D. Introduction to the open source PV LIB for python photovoltaic system modelling package. In: 2014 IEEE 40th photovoltaic specialist conference (PVSC); 2014. p. 0170–4. http://dx.doi.org/10.1109/PVSC.2014.6925501.

[23] Louwen A, de Waal AC, Schropp REI, Faaij APC, van Sark WGJHM. Comprehensive characterisation and analysis of PV module performance under real operating conditions. Prog Photovoltaics: Res Appl 2017;25(3):218–32. http://dx.doi.org/10.1002/pip.2848. pip.284.

[24] Moraitis P, van Sark WG. Operational performance of grid-connected PV systems. In: 2014 IEEE 40th photovoltaic specialist conference (PVSC), IEEE; 2014. http://dx.doi.org/10.1109/pvsc.2014.6925308.

[25] Liander NV.Liander open data; 2016. URL < https://www.liander.nl/over-liander/innovatie/open-data/data > .

[26] Litjens G, Worrell E, van Sark W. Influence of demand patterns on the optimal orientation of photovoltaic systems. Sol Energy 2017;155:1002–14. http://dx.doi.org/10.1016/j.solener.2017.07.006.

[27] Hintze JL, Nelson RD. Violin plots: a box plot-density trace synergism. Am Stat 1998;52(2):181–4. http://dx.doi.org/10.2307/2685478.

[28] Dee DP, Uppala SM, Simmons AJ, Berrisford P, Poli P, Kobayashi S, et al. The era-interim reanalysis: configuration and performance of the data assimilation system. Quart J Roy Meteorol Soc 2011;137(656):553–97. http://dx.doi.org/10.1002/qj.828.

[29] Ineichen P, Perez R. A new airmass independent formulation for the Linke turbidity coefficient. Sol Energy 2002;73(3):151–7. http://dx.doi.org/10.1016/S0038-092X(02)00045-2.

[30] Hoppmann J, Volland J, Schmidt TS, Hoffmann VH. The economic viability of battery storage for residential solar photovoltaic systems – a review and a simulation model. Renew Sustain Energy Rev 2014;39:1101–18. http://dx.doi.org/10.1016/j.rser.2014.07.068.

[31] SMA Solar Technology AG. Sunny boy storage 2.5; 2017. URL < https://www.sma.de/en/products/battery-inverters/sunny-boy-storage-25.html#Downloads-236248 > .

[32] Tesla Motors, Inc. Tesla Motors, Inc. Powerwall product homepage; 2016. URL < http://www.teslamotors.com/nl_NL/powerwall > .

[33] Weniger J, Tjaden T, Quaschning V. Sizing of residential PV battery systems. Energy Proc 2014;46:78–87. http://dx.doi.org/10.1016/j.egypro.2014.01.160.

[34] Jordan DC, Kurtz SR, VanSant K, Newmiller J. Compendium of photovoltaic degradation rates. Prog Photovoltaics: Res Appl 2016;24(7):978–89. http://dx.doi.org/10.1002/pip.2744. pIP-15-244.R.

[35] Truong Cong Nam, Naumann Maik, Karl Ralph Ch, Müller Marcus, Jossen Andreas, Hesse Holger C. Economics of residential photovoltaic battery systems in Germany: the case of teslas powerwall. Batteries 2(14). http://dx.doi.org/10.3390/batteries2020014.

[36] Downing S, Socie D. Simple rainflow counting algorithms. Int J Fatigue 1982;4(1):31–40. http://dx.doi.org/10.1016/0142-1123(82)90018-4.

[37] Rosenkranz CA, Köhler U, Liska J-L. Modern battery systems for plug in hybrid vehicles. In: 23rd International battery, hybrid and fuel cell electric vehicle symposium and exhibition; 2007. p. 650–61.

[38] Vaz A, Elsinga B, van Sark W, Brito M. An artificial neural network to assess the impact of neighbouring photovoltaic systems in power forecasting in Utrecht, the Netherlands. Renew Energy 2016;85:631–41. http://dx.doi.org/10.1016/j.renene.2015.06.061.

[39] Iwafune Y, Yagita Y, Ikegami T, Ogimoto K. Short-term forecasting of residential building load for distributed energy management. In: 2014 IEEE international energy conference (ENERGYCON), IEEE; 2014. http://dx.doi.org/10.1109/energycon.2014.6850575.

[40] Ryu S, Noh J, Kim H. Deep neural network based demand side short term load forecasting. In: 2016 IEEE international conference on smart grid communications (SmartGridComm), IEEE; 2016. http://dx.doi.org/10.1109/smartgridcomm.2016.7778779.

[41] Luthander R, Widén J, Nilsson D, Palm J. Photovoltaic self-consumption in buildings: a review. Appl Energy 2015;142:80–94. http://dx.doi.org/10.1016/j.apenergy.2014.12.028.

[42] Beck T, Kondziella H, Huard G, Bruckner T. Assessing the influence of the temporal resolution of electrical load and PV generation profiles on self-consumption and sizing of PV-battery systems. Appl Energy 2016;173:331–42. http://dx.doi.org/10.1016/j.apenergy.2016.04.050.

[43] van Sark WG, Bosselaar L, Gerrissen P, Esmeijer K, Moraitis P, van den Donker M, et al. Update of the Dutch PV specific yield for determination of PV contribution to renewable energy production: 25% more energy. In: WIP-renewable energies, Munich, Germany; 2014. p. 4095–7. http://dx.doi.org/10.4229/EUPVSEC20142014-7AV.6.43.

[44] Parra D, Gillott M, Norman SA, Walker GS. Optimum community energy storage system for PV energy time-shift. Appl Energy 2015;137:576–87. http://dx.doi.org/10.1016/j.apenergy.2014.08.060.

[45] Klaassen E, Kobus C, Frunt J, Slootweg J. Responsiveness of residential electricity demand to dynamic tariffs: experiences from a large field test in the Netherlands. Appl Energy 2016;183(Suppl C):1065–74. http://dx.doi.org/10.1016/j.apenergy.2016.09.051.

[46] Widén J. Improved photovoltaic self-consumption with appliance scheduling in 200 single-family buildings. Appl Energy 2014;126:199–212. http://dx.doi.org/10.1016/j.apenergy.2014.04.008.

[47] Staats M, de Boer-Meulman P, van Sark W. Experimental determination of demand side management potential of wet appliances in the Netherlands. Sustain Energy Grids Netw 2017;9:80–94. http://dx.doi.org/10.1016/j.segan.2016.12.004.

[48] van der Kam M, van Sark W. Smart charging of electric vehicles with photovoltaic power and vehicle-to-grid technology in a microgrid; a case study. Appl Energy 2015;152:20–30. http://dx.doi.org/10.1016/j.apenergy.2015.04.092.

[49] Salpakari J, Lund P. Optimal and rule-based control strategies for energy flexibility in buildings with PV. Appl Energy 2016;161:425–36. http://dx.doi.org/10.1016/j.apenergy.2015.10.036.

[50] Stephan A, Battke B, Beuse MD, Clausdeinken JH, Schmidt TS. Limiting the public cost of stationary battery deployment by combining applications 2016:1;16079. http://dx.doi.org/10.1038/nenergy.2016.79.